Master Thesis report

Virology and Immunology laboratory – GIGA institute

Student : Maxime Dubois – Promoter : Catherine Sadzot

Engineering and characterization of an Oncolytic Herpes Simplex Virus type 1 armed with P2G to disrupt CXCR4 pathway in Glioblastoma Multiforme

As part of the Master in Biochemistry & cellular and molecular biology, research focus, 2020 – 2021

ULiege

Faculty of Sciences, Departments of Life Sciences

Master Thesis report

Virology and Immunology laboratory – GIGA institute

Student : Maxime Dubois – Promoter : Catherine Sadzot

Engineering and characterization of an Oncolytic Herpes Simplex Virus type 1 armed with P2G to disrupt CXCR4 pathway in Glioblastoma Multiforme

As part of the Master in Biochemistry & cellular and molecular biology, research focus, 2020 – 2021

ULiege

Faculty of Sciences, Departments of Life Sciences

Table of contents

Acknowledgment

I would like to express my deepest thanks to my promoter, Mrs. Catherine Sadzot, for allowing me to work on a project in which I had a great interest, and for her precious advice at every step of my master thesis. I am especially grateful for her guidance and the help she provided me in developing a critical approach to my own work.

This project also would not have been possible without Paolo D'Arrigo and Judit Sanchez, who introduced me to it and took the time to explain to me the numerous properties of glioblastoma multiforme and oncolytic viruses. I would like to thank them as well for their patience and for all the practical aspects of laboratory work they taught me. I would like to acknowledge the assistance of Cédric Lassence, Marielle Lebrun, Mégane Jassin and all members of the different laboratories in everyday work throughout my internship.

Finally, I would like to express my gratitude to my girlfriend, my family and my friends who supported me throughout my studies and patiently listened to me trying to explain my project.

List of abbreviations

(S)gG	(Soluble) glycoprotein G
3-OST HS	3-O-Sulfonated derivates of Heparan Sulfate
AC	Adenylyl Cyclase
AGE	Agarose Gel Electrophoresis
APS	Ammonium Persulfate
BAC	Bacterial Artificial Chromosome
BBB	Blood Brain Barrier
BSA	Bovine Serum Albumin
CAF	Cancer Associated Fibroblasts
CC	Corpus Callosum
Cm	Chloramphenicol
CMV	Cytomegalovirus
Cp	Crossing Points
CSC	Cancer Stem Cell
CTL	Cytotoxic T Lymphocytes
CXCL12	CXC chemokine Ligand 12
CXCR4	CXC chemokine Receptor 4
DMEM	Dulbecco's Modified Eagle Medium
DNA	Deoxyribonucleic Acid
DO_{600}	Optical Density at 600 nm
E	Early
E. coli	*Escherichia coli*
E-cadherin	Epithelial cadherin

ECL	Electro-Chemiluminescence
ECM	Extracellular Matrix
EDTA	Ethylenediaminetetraacetic acid
EGF	Epidermal Growth Factor
EIF2a	Eukaryotic Initiation Factor 2a
ELISA	Enzyme-Linked Immunosorbent Assay
EMT	Epithelial-to-Mesenchymal Transition
ERK1/2	Extracellular Regulated Kinase ½
FACS	Fluorescence Activated Cell Sorting
FBS	Foetal Bovine Serum
gB, gC, gD, gH, gL	glycoprotein B, C, D, H, L
GBM	Glioblastoma Multiforme
GFP	Green Fluorescent Protein
GIC	Glioblastoma Initiating Cells
GL261 N+	GL261 Nectin positive
GM-CSF	Granulocyte–macrophage colony-stimulating factor
GPCR	G-Protein Coupled Receptor
GRK	GPCR Kinase
GSC	Glioblastoma Stem Cells
hFGF	human Fibroblast Growth Factor
HG	High Glucose
HH	Hedgehog signalling pathway
HIF	Hypoxia Inducible Factors
HSPG	Heparan Sulphate Proteoglycan
HSV-1	Herpes Simplex Virus 1

HSV-2	Herpes Simplex Virus 2
HVEM	Herpesvirus Entry Mediator
ICAM-1	Intercellular Adhesion Molecule 1
ICP	Infected Cell Protein
IE	Immediate Early
IF	Immunofluorescence
IFN	Interferon
IFP	Intermediate filaments Proteins
IL-8	Interleukin 8
IP3	Inositol 1,4,5 trisphosphate
IRF	Interferon Regulatory Factor
Jet PEI	Jet Polyethyleneimine
Kana	Kanamycin
Kd	Dissociation Constant
L	Late
LB	Lysogeny Broth
MAPK	Mitogen-Activated Protein Kinase
MC	Mast Cell
MDA5	Melanoma Differentiation-Associated gene 5
MDSC	Myeloid-Derived Suppressor Cell
MET	Mesenchymal-to-Epithelial Transition
MHC	Major Histocompatibility Complex
MMP	Matrix Metalloproteases
MOI	Multiplicity Of Infection
MSC	Mesenchymal Stem Cell

N-cadherin	Neural cadherin
NFκB	Nuclear Factor-kappa B
NPC	Neural Progenitor Cell
NSC	Neural Stem Cell
NTP	Nucleoside Triphosphate
oHSV	Oncolytic Herpes Simplex Virus 1
oHSV-P2G	Oncolytic Herpes Simplex Virus 1 expressing P2G transgene
ON	Overnight
OS	Overall Survival
OV	Oncolytic Virus
P2G	CXCL12 mutated chemokine (2 amino acid from proline to glycine)
PAGE	Polyacrylamide Gel Electrophoresis
PAMPs	Pathogen-Associated Molecular Patterns
PBS	Phosphate Buffer Saline
PBS-T	Phosphate Buffer Saline-Triton
PCR	Polymerase Chain Reaction
PEDF	Pigment Epithelium-Derived Factor
pEF1a	promoter eukaryotic translation Elongation Factor 1 alpha
PFS	Progression Free Survival
PI3K	Phosphoinositide 3-Kinase
PIP2	Phosphatidylinositol 4,5-bisphosphate
PKR	Protein Kinase RNA-regulated
PLC	Phospholipase C
RIGI	Retinoic acid-Inducible Gene I
RNA	Ribonucleic Acid

Rpm	Rotation per minute
RR	Ribonucleotide Reductase
RT	Room Temperature
RT-qPCR	Reverse Transcription-quantitative Polymerase Chain Reaction
SDF-1	Stromal cell-Derived Factor 1
SDS	Sodium Dodecyl Sulfate
STAT3	Signal Transducers and Activators of Transcription 3
SVZ	Sub Ventricular Zone
TAE	Tris-Acetate-EDTA
TAP	Transporter associated with Antigen Processing
TBS-T	Tris-Buffered Saline-Tween
TE	Tris-EDTA
TEMED	N, N, N, N-Tetramethylethylenediamine
TGF-β	Transforming Growth Factor β
TK	Thymidine Kinase
TMZ	Temozolomide
TNFR	Tumour Necrosis Factor Receptor
Treg	regulatory T cell
T-VEC	Talimogene laherparepvec
US11	Unique Short region 11
VEGF	Vascular Endothelial Growth Factor
VP-SFM	Virus Production-Serum Free Medium
VZV	Varicella Zoster Virus
WB	Western Blotting
WHO	World Health Organization

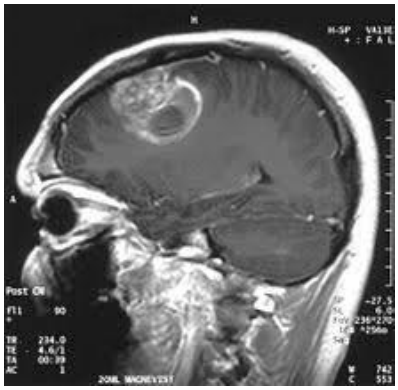

Figure 1 : Glioblastoma (astrocytoma) WHO grade IV. MRI sagittal view, post contrast. 15 years-old boy. (Christaras. A, 2006)

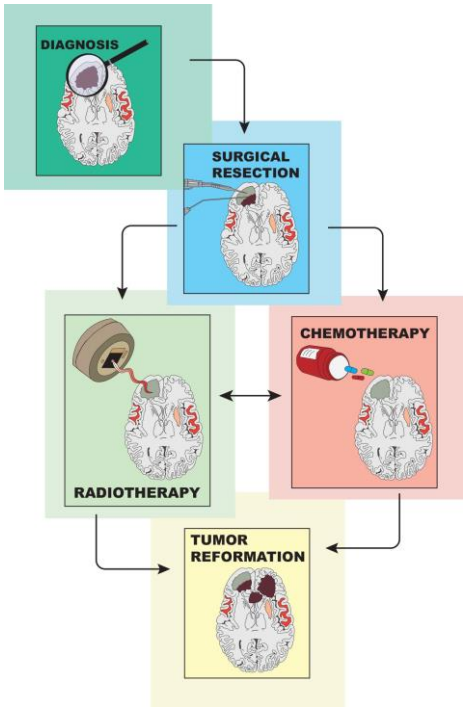

Figure 2 : Current standard therapies after GBM diagnosis. Current standard therapies consist in maximal surgical resection followed by chemo- or radio-therapy and are often ineffective mainly due to systematic resurgences and tumour reformation. (Paolo D'Arrigo, Post-doc)

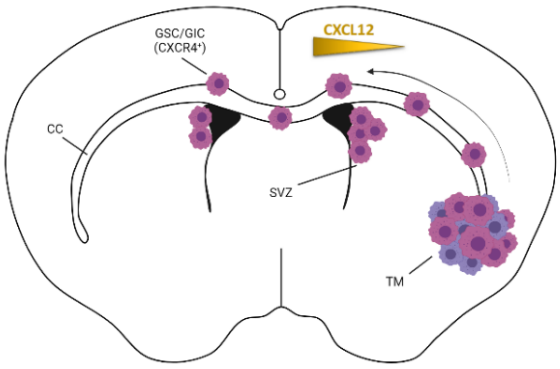

Figure 3 : GSCs/GICs migration from the tumour mass to the SVZ along CXCL12 gradient. GSCs/GICs are specific $CXCR4^+$ undifferentiated glioblastoma cells with stem-like features and display the ability to initiate the formation of new tumours after treatment. CXCR4/CXCL12 pathway contributes to their properties as well as their migration towards specific brain niches such as the SVZ. CC, Corpus Callosum; SVZ, Sub-Ventricular Zone; TM, Tumour Mass. *Created with BioRender.com*

I. Introduction

1. Glioblastoma multiforme (GBM) and therapeutic strategies

Glioblastoma multiforme is the most common form of gliomas which makes it the most frequent subtype of primary brain tumours.[1–4] Indeed, GBM represents around 60% of reported human brain tumours.[5]

GBMs are classified as a high-grade astrocytoma (WHO, grade IV), which also makes them the most aggressive and lethal form of primary brain tumours.[1–4] This leads to an overall median patient survival of around 15 months in adults.[1–4] **(*Figure 1*)**

GBMs are characterized by considerable proliferation of cells as well as extensive hypoxia, angiogenesis, and invasion.[4] Like other gliomas, GBMs also show a certain disruption of the blood brain barrier (BBB) related to an abnormal vasculature with important leakiness. This further leads to extreme invasiveness promoting expansion of GBM.[3] By contrast with low-grade gliomas, GBMs express severe microvascular hyperplasia and increased necrosis. A feature that is relatively unique to GBMs is that the necrotic foci are surrounded by pseudopalisading cells. The latter are extensively hypoxic, therefore expressing the hypoxia-inducible factor (HIF-1). Besides, they also produce important quantities of proangiogenic factors such as Vascular Endothelial Growth Factor (VEGF) and IL-8.[4,6]

Current standard therapies after glioblastoma multiforme diagnosis consist in maximal resection, when surgery is feasible, followed by radiotherapy and chemotherapy with temozolomide (TMZ).[7–9] The inefficacy of these strategies are mainly due to systematic recurrences giving rise to even more aggressive tumours.[4,10] **(*Figure 2*)**

These relapses were attributed to undifferentiated glioblastoma cells which exhibit stem-like features and are able to initiate the formation of a new tumour after treatment. For this reason, they are named either glioblastoma stem-like cells (GSCs) or glioblastoma initiating cells (GICs). Furthermore, these cells are able to migrate to specific niches, which consist in particular pro-tumoral microenvironment in the brain. **(*Figure 3*)** In this way, GSCs avoid resection, maintain their stemness features and are rendered resistant to radiotherapy.[1,2,4] Those cells are recognisable by some markers such as CD133, Nestin and CXCR4 and have the ability to proliferate into 3D neurospheres *in vitro*.[1,11]

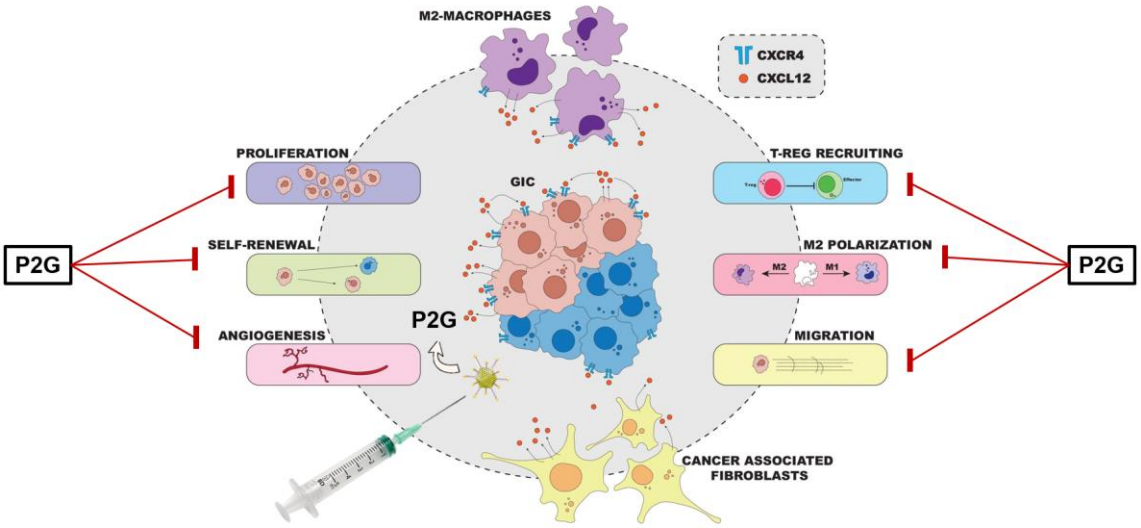

Figure 4 : CXCR4/CXCL12 pathway in the GBM microenvironment and oHSV-P2G treatment. (i) Activation of the CXCR4/CXCL12 signalling pathway resulting from autocrine and paracrine stimulation of GICs, M2-like macrophages, and CAFs, results in the creation of a specific GBM microenvironment around the tumour mass. This microenvironment stimulates GICs proliferation, self-renewal and migration, as well as angiogenesis, M2 polarization and T-regs recruiting. (ii) Direct injection of oHSV-P2G at the GBM tumour site allow infection of tumour cells and continuous production of P2G which is expected to disrupt CXCR4/CXCL12 pathway-mediated GBM microenvironment features. (Paolo D'Arrigo, Post-doc)

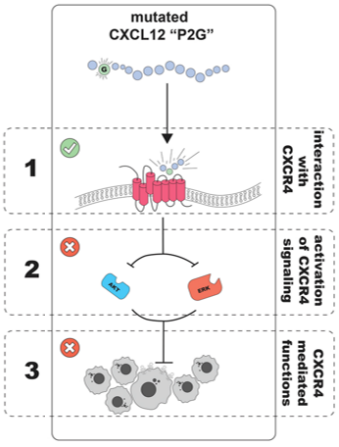

Figure 5 : Mutated CXCL12 "P2G", a CXCL12 competitive inhibitor. Mutated CXCL12 "P2G" (P2G, second amino acid changed from a proline to a glycine) interacts with CXCR4 but is unable to activate downstream CXCR4 signalling and CXCR4 mediated functions. Thus, P2G can act as a potent competitive inhibitor of CXCL12 in GBM microenvironment. (Paolo D'Arrigo, Post-doc)

In the light of the above statements, it is critical to find new strategies to target those GSCs, to impair their migrating and angiogenic abilities, and to disturb GBM microenvironment. The migration of GSCs towards specific niches, namely the Sub Ventricular Zone (SVZ) of the brain, was shown to be mediated by a CXCL12 chemokine gradient attracting the $CXCR4^+$ GSCs.[1] **(*Figure* 3)** Inside the tumour mass, $CXCR4^+$ GSCs as well as other non-tumour cells are in fact also able to produce CXCL12 contributing to the creation of a specific pro-tumoural microenvironment at the tumour site, driven by CXCL12/CXCR4 pathway-related autocrine and paracrine stimulation. This microenvironment promotes tumour cell self-renewal, proliferation, and migration, as well as tumour angiogenesis, radioresistance and pro-tumoral immune modulation.[1-4,11–14] **(*Figure 4, i*)**

CXCL12/CXCR4 pathway can already be targeted by FDA-approved drugs like AMD3100 (Plerixafor, Mozobil™), as it was assessed for various cancers including glioblastoma.[15–17] However, AMD3100 still faces several issues as a therapeutic molecule. Indeed, the blood brain barrier has a limited permeability for this inhibitor which, mroeover lacks target specificity. Furthermore, systemic circulation of AMD3100 prior to transit through the BBB is also an issue.[18] Systemic circulation of CXCR4 inhibitors is indeed a problem as $CXCR4^+$ cells exists all around the body (endothelial cells, hematopoeitic stem cells, neural stem/progenitor cells, blood and immune cells) and this pathway is involved in tissue homeostasis and cellular traficking.[19] Moreover, targeting specificity inside the brain is important as neuronal stem cells are known to express significant levels of CXCR4.[20,21] There is therefore a need for a more targeted vector to deliver CXCR4 antagonists.

During this master thesis, an oncolytic Herpes Simplex Virus type 1 (oHSV) modified to specifically replicate in tumour cells while sparing normal cells will be used.[22–27] This oHSV will be armed to express, under control of the strong mammalian promoter pEF1a, a mutated form of CXCL12 called P2G (second proline of the CXCL12 cytokine changed for a glycine). P2G is able to bind CXCR4 receptor with high affinity, though around 3 times lower than CXCL12 affinity towards CXCR4, but unable to activate the downstream signalling.[28] P2G could thus act as a competitive inhibitor of the CXCL12/CXCR4 pathway. **(*Figure 5*)** The aim of this master thesis is to engineer the above-mentioned oHSV producing P2G (oHSV-P2G) and to characterise its impact on migration abilities of human (T08, T013, GB138) primary cells and murine (GL261 N^+) cell lines *in vitro* (P2G interacting with both human and murine CXCR4). The characterisation in murine cell lines is important in the prospect of future *in vivo* analysis in GBM mouse models. The use of this immunocompetent model is essential for the investigation of the GBM microenvironment, including the immune response. **(*Figure 4, ii*)**

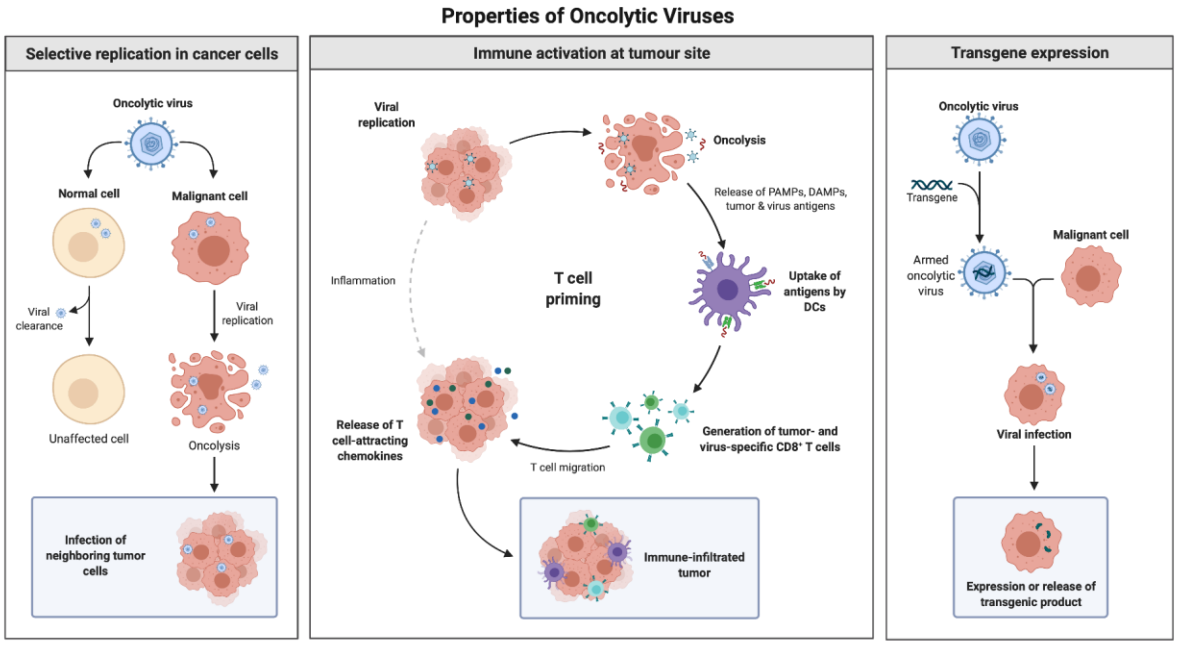

Figure 6 : Oncolytic viruses properties. Oncolytic viruses (OVs) are relatively selective towards tumour cells vs healthy cells. This give them the ability to leave healthy cells undamaged while specifically infecting tumour cells and causing their lysis. Viral infection and continuous targeted killing of tumour lead to local inflammation and disruption of pro-tumoral microenvironment, infection of more tumour cells, release of tumour antigens and systemic anti-tumour immune response. OVs can also be armed with transgenes and produce transgenic products at the site of infection.[29]

2. Oncolytic viruses

2.1. Description

Standard therapies against glioblastoma have a limited efficacy mainly due to recurrence of tumours after treatment. Due to the diffuse aspect of the tumour, total resection is almost impossible and surgery usually leaves malignant cells behind. Moreover, some tumour cells become resistant to chemo- and radiotherapy and escape, thus, these post-surgery treatments. Therefore, a continual targeted killing of tumour cells will be benificial.[26] Oncolytic viruses (OVs) are viruses from various families, which naturally selectively infect and replicate in tumour cells or are genetically engineered to target the tumour cells or a sub-population of these cells and cause their lysis. As biological agents, OVs are able to replicate and spread throughout the tumour. In addition, viral infection and tumour cell lysis will release viral/tumour specific antigens and neoantigens resulting in a systemic anti-tumorigenic response involving both the innate and adaptive immune response (e.g. cytokines, tumour-specific T cells).[22,23,26,29] **(*Figure 6*)**

Besides being engineered to target tumour cells or specific sub-population of these cells, OVs can be armed by introducing heterologous DNA in their genome sequence to force infected cells to produce anti-tumoral drugs, notably cytokines, apoptosis signals, antiangiogenetic molecules.[23] **(*Figure 6*)**

As a result, this production of therapeutic molecules at the tumour site by the infected cells, combined with local inflammation caused by viral infection and tumour antigens, will potentially convert the tumour microenvironment from pro- to anti-tumoral .[22,29] Among the various families of viruses that can be used as OVs, which are under development or currently ongoing analysis and clinical trials, herpesviruses particularly stand out.

2.2. Oncolytic Herpes Simplex Virus-1 (oHSV)

2.2.1. HSV-1

HSV-1 is a large double-stranded DNA enveloped virus, like all viruses from the Herpesviridae family. Specifically, HSV-1 belongs to the alphaherpesvirinae subfamily comprising notably HSV-2, and the Varicella zoster virus (VZV).[30] The Herpesviridae are ubiquitous, cause a wide range of diseases and can establish a lifelong latency in their host. Precisely, HSV-1 is known for commonly causing mucocutaneous lesions in the oral or genital regions but can also lead to encephalitis and meningitis in rare circumstances. Indeed, the prominent targets of the virus are epithelial and neural cells, even though various cell types such as lymphocytes and fibroblasts can be infected.[30]

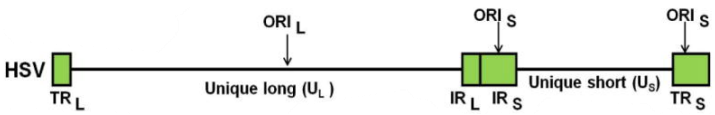

Figure 7 : HSV-1 genome organization. HSV-1 genome is a monopartite, linear, dsDNA molecule of 152 kb. It is organized in unique short and long sequences (U_S, U_L) framed by terminal/internal inverted repeated sequences of the long or short region (TR_L/IR_L, TR_S/IR_S). It also contains two origin of replication in the repeated sequences of the short region (ORI_S) and one in the U_L (ORI_L).[31]

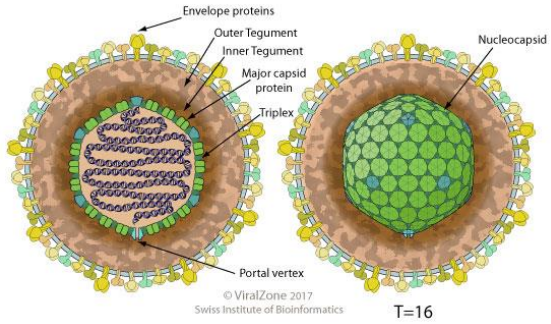

Figure 8 : HSV-1 virion structure. The 150-200 nm viral particle consists of an icosahedral nucleocapsid in which the genome is encapsulated. This nucleocapsid is surrounded by several layers of proteins forming the tegument itself covered by a phospholipidic viral envelope dotted with glycoproteins.[32]

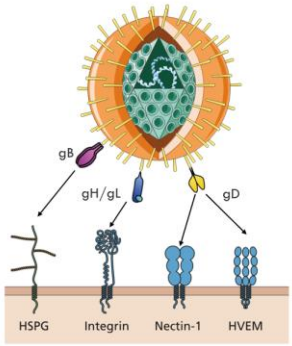

Figure 9 : HSV-1 glycoproteins in virus entry. The viral envelope contains several glycoproteins involved in virus entry into host cells. gD, gH-gL, and gB are involved in cll entry through interaction with various receptors expressed at the cell surface (Nectin-1, HVEM, Integrin, HSPG). Upon binding of gD, gH-gL and gB will undergo conformational changes leading to the fusion of the viral envelope and the cell plasma, and to the entry of the virus in the host cell cytoplasm. (Judit Sánchez Gil, PhD)

HSV-1 large particle carries a monopartite, linear, dsDNA genome of 152 kb. HSV-1 genome is organized in unique short and long sequences (U_S, U_L) both framed by terminal/internal inverted reiterated sequences. The genome contains two origins of replication in the repeated sequences of the short region (ORI_S) and one in the U_L (ORI_L).[31] **(*Figure 7*)** The 150-200 nm viral particle consists of an icosahedral nucleocapsid in which the genome is encapsulated. This nucleocapsid is surrounded by several layers of proteins forming the tegument itself protected by a phospholipidic viral envelope.[32] **(*Figure 8*)** The viral envelope contains glycoproteins which are essential in the first steps of the infectious cycle, being important for attachment with cellular components, fusion between the cell membrane and the viral envelope, as well as entry. These glycoproteins and their receptors on host cell determine, thus, which cells are susceptible to be infected.[30] The receptor-binding proteins supporting HSV-1 attachment and entry are gC, the gD homodimer, as well as the gH-gL heterodimer and the trimeric fusion protein gB, which are both conserved among Herpesviridae.[30,33] **(*Figure 9*)**

gD is the main factor determining the infected cell type. It binds several classes of receptors, namely nectins, 3-O-sulfonated derivatives of heparan sulfate (3-OST HS) and herpesvirus entry mediator (HVEM) which belongs to the tumour necrosis factor (TNFR) family. Nectin is the major ligand for alphaherpesviruses while HVEM and 3-OST HS are more specific to HSVs. Significantly, nectin 1 is expressed in neuronal tissues which consist in one of the preferential targets of alphaherpesviruses and HVEM is expressed on immune cells which are another known target of HSVs.[30] gH-gL and gB, which binds respectively integrins and HSPG, will undergo conformational changes upon binding of gD to its specific receptors. These conformational changes will eventually activate gB which is responsible for the fusion between the viral envelope and the host cell membrane, resulting in entry of the virus in the host cell cytoplasm.[30] **(*Figure 9*)**

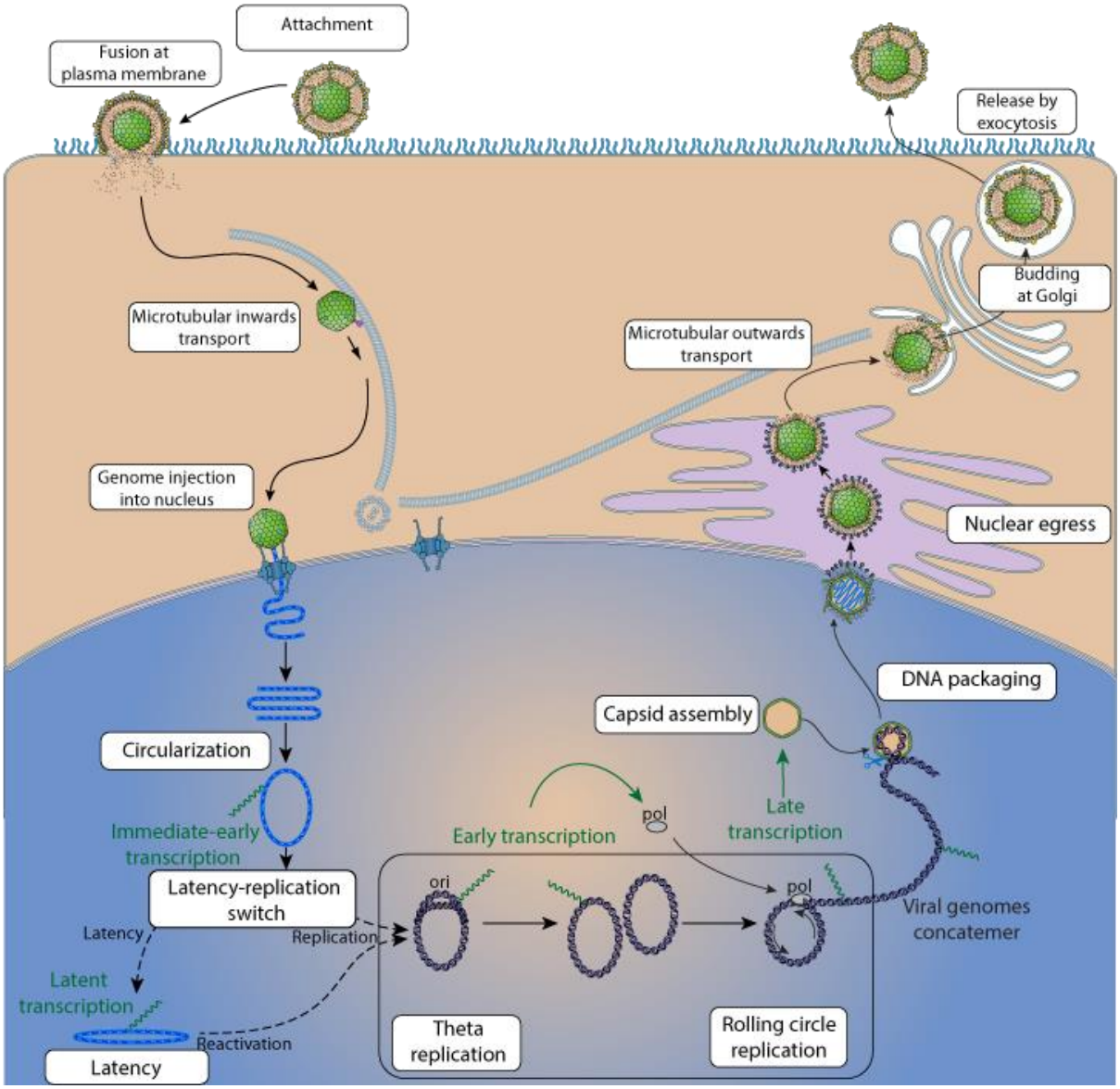

Figure 10 : HSV-1 infectious cycle. Glycoproteins inside the viral envelope are important for attachment with cellular components, fusion between the cell membrane and the viral envelope, as well as entry. Subsequently, the viral capsid is transported along microtubules to a nuclear pore and inject the genome into the cell nucleus. The genome then rapidly circularizes before IE and E genes transcription. Products of E genes trigger theta replication of the circular genome from one of the origins of replication. Afterwards, viral DNA is synthesise by rolling circle as linear concatemer copies, later cleaved by a site-specific viral endonuclease. Finally, L genes responsible for viral assembly and cell lysis are transcribed. Viral assembly occurs in nuclear viral factories before nuclear egress through the inner lamella of the nuclear envelope, previously dotted with the viral glycoproteins (temporary primary envelope). Viral particles eventually transit from the endoplasmic reticulum along microtubules towards the Golgi (final secondary envelope) before their release by exocytosis. Instead of entering this lytic replication cycle, a latency-replication switch can occur before theta replication. Some genes can still be transcribed during latency and reactivation can occur at any time to re-enter the lytic replication cycle.[34]

Subsequently, the viral capsid is transported by motor proteins (kinesin, dynein) along microtubules to a nuclear pore in order to inject the genome into the cell nucleus thanks to a recruited cellular protein machinery. The genome then rapidly circularizes via its terminal repeated sequences before starting the three consecutive transcription cycles.[32] Indeed, viral genes are divided into three categories: Immediate Early (IE), Early (E), and Late (L) genes, depending on the stage of the virus cycle during which they are transcribed by host polymerase II. IE genes allow evasion from the immune system and preparation for viral replication, in which E genes will be involved.[25,26] Thus, the products of E genes will start by triggering a first round of circular genome amplification by bidirectional replication (Theta replication) from one of the origins of replication. Afterwards, viral DNA will be synthesised by rolling circle as linear concatemer copies which will later be cleaved by a site-specific viral endonuclease.[32] Finally, L genes (which encode envelope glycoproteins and capsid/tegument proteins) are transcribed and will be responsible for viral assembly and cell lysis.[25,26] Viral assembly consists in the formation of large icosahedral empty capsids relying on scaffolding proteins acting as chaperones, followed by packaging of the viral DNA inside the empty capsids via the portal system. This assembly occurs in nuclear viral factories before nuclear egress through the inner lamella of the nuclear envelope which has been previously dotted with the viral glycoproteins (temporary primary envelope). Viral particles eventually transit from the endoplasmic reticulum along microtubules towards the Golgi (final secondary envelope) before their release by exocytosis.[32,34] **(*Figure 10*)**

Instead of entering this lytic replication cycle, a latency-replication switch can occur before the bidirectional replication. Some genes can still be transcribed during latency and reactivation can occur at any time to re-enter the lytic replication cycle.[32,35] **(*Figure 10*)**

2.2.2. HSV-1, suited as oncolytic virus

HSV-1 virus was suggested to be an interesting candidate for the development of oncolytic viruses, notably as it is easily engineered and produce an immune response while remaining safe.[21-26]

Indeed, HSV-1 is a double-stranded DNA virus with a 150-kb-long genome which encodes 84 genes which are not all essential for replication.[25,26] HSV-1 genome is thus easily engineered through mutations, deletions, or addition of transgenes without critical impact on viral growth.[25,26] HSV-1 has a rapid lytic cycle, infects a wide variety of cell types, and is able by itself to induce strong innate and adaptive immune response.[22,23,25] This immune stimulation could serve to disrupt the immunosuppressive tumour microenvironment.[24]

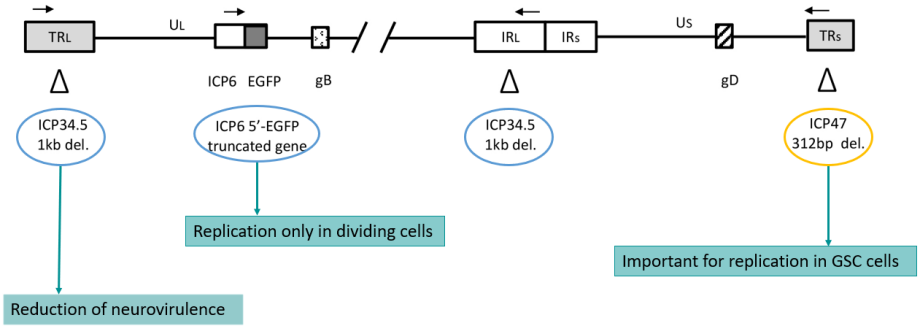

Figure 11 : oHSV genome modifications. oHSV engineering implied ICP 34.5 (two copies in the genome), ICP6 and ICP47 deletion for reduction of neurovirulence, selectivity towards dividing cells, and towards GSCs, respectively. (Judit Sánchez Gil, PhD)

Despite these features, HSV-1 remains a safe vector for oncolytic therapies, notably as it is already ubiquitous in human populations.[22,23,25] In fact, this ubiquity raised a question about a potential immunity against *de novo* infection in humans. However, as it was already suggested by usual viral reactivation from the latent stage in immunocompetent individuals, early animal models confirmed that re-infection was not prohibited by pre-existing immunity (such as HSV-1 antibodies).[25] Furthermore, the risk of virus-mediated mutagenesis is low as the viral DNA, which exists as a circular episome within the nucleus, never incorporate into the host genome.[25] Finally, the viral infection can be easily controlled by anti-herpetic drugs (e.g. acyclovir).[22,23,25]

In fact, the first FDA-approval for an OV was for the oHSV talimogene laherparepvec (T-VEC), delivered in 2015, for the treatment of metastatic melanoma.[22,24] Currently, engineered HSV-1 oncolytic viruses (oHSV) are under investigation in numerous clinical trials including GBM.[22]

2.2.3. Design of HSV-1 as oncolytic virus

To be used as an oncolytic virus, HSV has to be genetically engineered to reduce neurovirulence and improve tumour specificity.[22] For this reason, HSV-1 genome has been cloned in a bacterial artificial chromosome (BAC). Indeed, this facilitated reliable heterologous recombination with foreign DNA sequences as well as introduction of the modifications necessary to reduce or inhibit infection and lysis of normal host cells and to favour the viral replication in tumour cells (e.g. deletion of genes encoding TK, ICP34.5, ICP6, ICP47)[22,23]. Subsequently, heterologous recombination are used to introduce a transgene coding for proteins able to induce or inhibit biological features or to modify the tumour microenvironment (e.g. addition of the transgene encoding GM-CSF).[24]

In this master's thesis, the used oHSV underwent deletion of the two genes encoding ICP34.5 (γ34.5, L), as well as deletion of the ICP6 (UL39, E) and ICP47 (US12, IE) encoding genes.[25,26] **(*Figure 11*)**

2.2.3.1. ICP34.5

ICP34.5 has been described as an essential neurovirulence factor essential for HSV pathogenicity and replication in normal cells. It is thus deleted to attenuate the virus.[25–27]

First, HSV ICP34.5 binds the autophagy protein Beclin 1 via its N-terminal domain and inhibits thereby its autophagy function. A mutant lacking the Beclin 1-binding domain of ICP34.5 demonstrates impaired ability to cause lethal encephalitis in mice.[24,37]

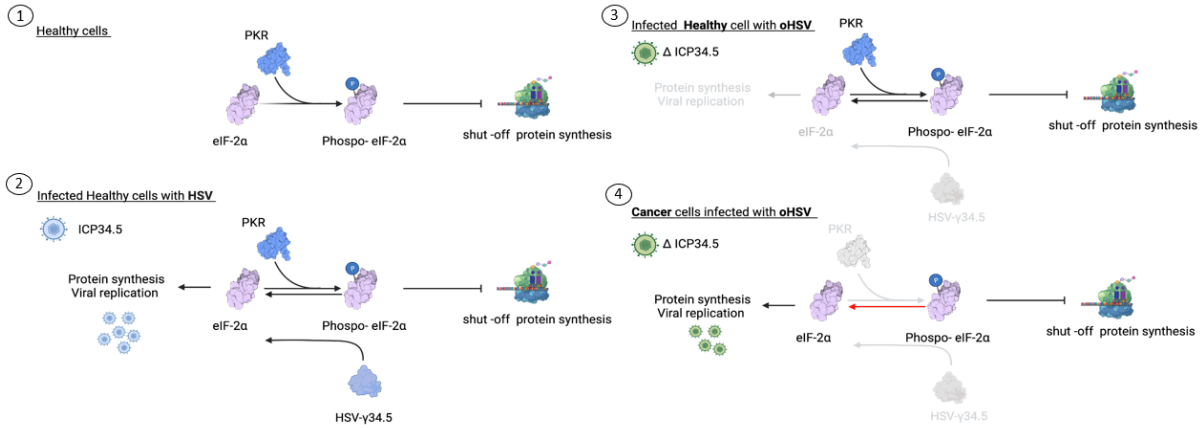

Figure 12 : Rationale for ICP34.5 deletion. Schematic representation of ICP34.5 function during oHSV infection and selective infection of PKR-depleted cancer cells by oHSV ΔICP34.5, decreasing neurovirulence. PKR activity leads to protein synthesis shut-off upon infection (1) but ICP34.5 is able to counteract PKR-mediated eiF2a phosphorylation (2). ICP34.5 deletion impairs viral replication in healthy cells (3) but allows replication in PKR-depleted cancer cells (4). (Judit Sánchez Gil, PhD)

Figure 13 : Rationale for ICP6 deletion. Schematic representation of ICP6 function during oHSV infection and selective infection of dividing cells by oHSV ΔICP6. Ribonucleotide Reductase (RR) is responsible for NTPs reduction into dNTPs for de novo DNA synthesis in dividing cells (1) but not active in non-dividing cells (2). ICP6 is a viral RR giving the ability to non-dividing cells to synthesise DNA de novo (3, 4). ICP6 deletion impairs viral replication only in non-dividing cells (5, 6). (Judit Sánchez Gil, PhD)

In addition, ICP34.5 inhibits the cellular protein kinase RNA-activated (PKR) pathway, thereby preventing interferon-induced viral protein synthesis shutoff. During infection, the presence of pathogen-associated molecular patterns (PAMPs), notably viral DNA, RNA or proteins, triggers the interferon system which leads to hampering of viral replication or cell apoptosis.[26,27] In healthy cells, the presence of dsRNA can be sensed by the Protein Kinase R (PKR), one of the protein over-expressed upon IFN signalling activation. Upon activation, PKR phosphorylates the translation initiation factor eIF2α which is thereby inactivated, leading to a global reduction in synthesis of proteins.[25–27] Nevertheless, in HSV-infected cells, this protein synthesis shut off is reversed by the interaction of ICP34.5 with the protein phosphatase 1 (PP1α) and eIF2α via its C-terminal domain, thereby restoring the expression of viral proteins.[25–27] Even though γ34.5 is a Late gene, ICP34.5 is a tegument protein delivered upon virus entry and is thus directly active upon entry, allowing HSV to evade the host immune response. Tumour cells are known to be deficient in PKR and in overall control of translation, antiviral or stress responses. oHSV ΔICP34.5 is thus able to selectively replicate in tumour.[25–27] **(*Figure 12*)**

Finally, ICP34.5 is also involved in disturbing the IFN system through inhibition of IRF3/7 phosphorylation by binding to TBK1 via its N-terminal domain.[24]

In the end, deletion of γ34.5 provides tumour selective replication and prevent serious neurologic infections.[25–27] However, these mutants are rendered hypersensitive to IFN inhibition and, unfortunately, replicate poorly in GSCs.[26]

2.2.3.2. ICP6

ICP6 is an E gene and thus important for viral replication. ICP6 is the large subunit of the viral ribonucleotide reductase (RR), which reduces ribonucleotides in deoxyribonucleotides (reduction of the 2'-COH group), and is thus essential to maintain a sufficient nucleotides pool for viral replication in normal cells. Indeed, viruses need a consequent nucleotides pool to replicate in host cells. This nucleotides pool is sufficient in proliferating tumour cells or in healthy dividing cells thanks to the activity of a cellular RR. However, the cellular RR is not active in healthy post-mitotic cells and, thus, the nucleotides pool is not sufficient for viral replication. As a result, the replication of oHSV deleted from ICP6 is limited to cycling cells but may also infect quiescent cancer cells with deficient cell cycle control (such as mutation of p16). Note that deletion of other genes involved in nucleotide metabolism like the thymidine kinase (TK) is also possible. However, the latter render the mutated oHSV less sensitive to antiherpetic nucleoside analogue drugs (e.g. acyclovir) which rely on TK inhibition. On the other hand, oHSV ΔICP6 is temperature sensitive and displays a hypersensitivity to those antivirals.[26] **(*Figure 13*)**

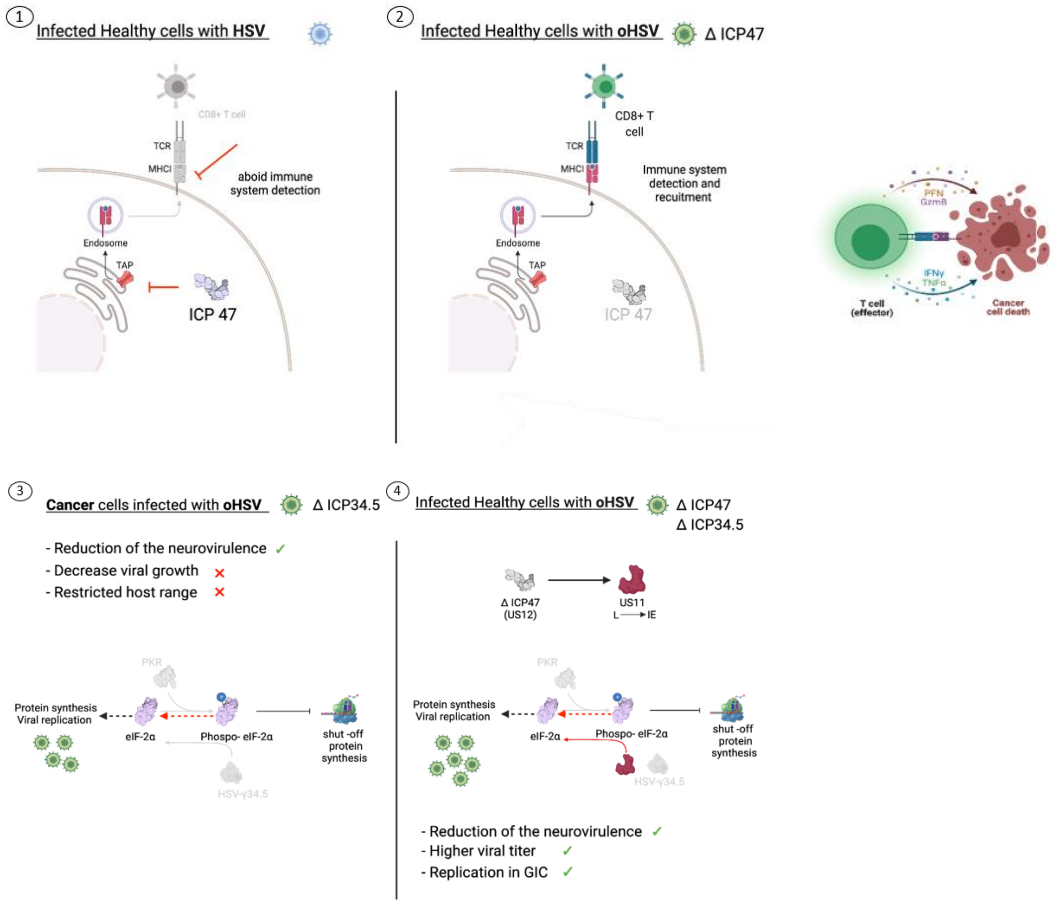

Figure 14 : Direct and indirect impact of ICP47 deletion. Schematic representation of ICP47 function during oHSV infection and selective infection of cancer cells by oHSV ΔICP47. ICP47 role in oHSV infection is to inhibit TAP activity to prevent viral antigen presentation to the host immune system via MHC-1 (1). ICP47 deletion allows detection of the infection by the immune system and recruitment of immune cells (effector T cells) to the infected tumour site (2). ICP34.5 is supposed to help in Phospho-eIF2a dephosphorylation and, thus, to prevent protein synthesis shut off. While decreasing neurovirulence and allowing viral replication in cancer cells, ICP34.5 deletion was still shown to be responsible for a decreased viral growth. (3). However, the impact of ICP34.5 deletion can be indirectly partly restored by ICP47 deletion. Indeed, ORF47 deletion put US11, a Late gene also able to preclude host shut off, under the control of ICP47 IE promoter. The IE expression of US11 can thus compensate the absence of ICP34.5, maintaining low neurovirulence but increasing viral replication in GICs. (4) (Judit Sánchez Gil, PhD)

2.2.3.3. ICP47

ICP47 interacts with the transporter associated with antigen processing (TAP) protein complex, thereby preventing peptide loading onto class 1 MHC molecules and subsequent MHC-1 expression on the surface of HSV-infected cells.[25,26] Deletion of orf47 restores immune recognition of tumour infected cells, enhancing immune response against infected tumour cells and anti-tumour immmunity.[25,26] Furthermore, the deletion of orf47 and US11 promoter (juxtaposed gene) places the US11 L gene under control of the ICP47 IE promoter.[25,26] This mutation is highly important as it restores the replication of oHSV ΔICP34.5 in tumour cells and increases tumour cell killing properties without reducing safety or selectivity.[25,26] In short, similarly as ICP34.5, US11 is involved in disturbing the cellular antiviral response by inhibiting PKR phosphorylation of EIF2α and RNA-mediated immune response. Precisely, US11 binds RIGI and MDA5, RNA sensors in the cytoplasm triggering IRF3 activation, inhibiting their activity.[26] **(*Figure 14*)**

During this master thesis, oHSV ΔICP34.5 ΔICP6 ΔICP47 will simply be called oHSV, used as a control and as a backbone for the generation of oHSV-P2G. The latter consists of oHSV in which a transgene coding for P2G (whose characteristics are described below) under control of the strong mammalian promoter pEF1a has been inserted.

3. CXCL12/CXCR4, a central pathway

3.1. CXCR4

CXCR4 is a seven-transmembrane domains G protein-coupled receptor (GPCR) that will activate several downstream signalling pathways upon stimulation by its ligand, CXCL12. CXCR4 is principally expressed by B/T-cells, macrophages and monocytes which are mainly present in bone marrow and lymphoid tissue. Thus, CXCL12 stimulation promotes particular phenotypes in CXCR4-expressing cells.[37–39] These phenotypes are involved in haematopoiesis, cardiac ventricular septum formation and vascularization of the gastrointestinal tract (regulating vascular branching and remodelling processes in endothelial cells). Besides, CXCL12-induced CXCR4 signalling is also involved in cerebellar development during embryogenic development of the brain and could mediate hippocampal-neuron survival.[41]

CXCR4 also has some functions which are not related to CXCL12 binding. Indeed, extracellular ubiquitin binding to CXCR4 also lead to downstream signalling resulting in increased intracellular Ca^{2+} and decrease cAMP levels. Bacterial lipopolysaccharide is also recognized by CXCR4 leading to an inflammatory response, notably to the secretion of TNF by monocytes. [41]

3.2. CXCL12

CXCL12 stands for C-X-C motif chemokine ligand 12 and is also called SDF1 (stromal cell-derived factor of the intercrine family). CXCL12 is secreted and acts as a growth factor, cytokine, or chemokine mainly active on T/B-lymphocytes and monocytes by interacting with its receptors CXCR4 and CXCR7. Indeed, CXCL12 plays several roles in embryogenic development, proliferation and growth of hematopoietic stem cells, tissue homeostasis, immune surveillance, as well as inflammation response, but also in tumour growth and metastasis (see 3.2.1. Pathogenic role).[40]

Precisely, CXCL12 was shown to stimulate lymphopoiesis of B cells, proliferation of bone marrow-derived B cell progenitors, and myelopoiesis in bone marrow. As a chemokine, CXCL12 is able to stimulate monocytes and T cells migration and decrease the β-2 integrins-mediated adherence of monocytes with ICAM-1 coated surfaces thanks to LYN kinase (Src family tyrosine kinase).[40] Furthermore, CXCL12 is important during embryonic development of the brain, notably in neurons from the foetal cerebellum.[41]

CXCL12 contains two receptor binding sites around the two cysteines (KPVSLSYR-CPC-RFFESH). RFFESH is involved in the initial contact with the receptor CXCR4. Even though this domain is important for optimal binding it absolutely needs KPVSLSYR for signalling activation by induced conformation change of CXCR4. In this N-terminal domain of CXCL12, only KP were shown to be directly involved in CXCR4 activation.[28] Indeed, removal of those two amino acids is sufficient to completely inhibit CXCR4 signalling upon binding while maintaining relative affinity of CXCL12 towards its receptor (SDF1 3-67).[28,36] The mutation of the 2nd proline to a glycine (P2G mutation) results in a complete inhibition of activation but only a 3-fold decrease of Kd. P2G is therefore able to act as a competitive inhibitor of the CXCL12/CXCR4 pathway acting in synergy with oHSV to increase immunogenicity and disturb the pro-tumoral microenvironment.[28]

3.3. CXCR4/CXCL12 signalling pathways

As described above, these CXCL12/CXCR4 signalling pathways have functions all over the body, notably in tissue homeostasis and cellular trafficking.[19] In the peripheral immune system, it promotes migration, survival, proliferation and intercellular communication of lymphocytes, monocytes, macrophages and neutrophiles.[37] In the central nervous system, it was shown to be involved in several activities, notably the proliferation and migration of NPCs towards injured areas where local astrocytes and endothelial cells up-regulate CXCL12 production.[37]

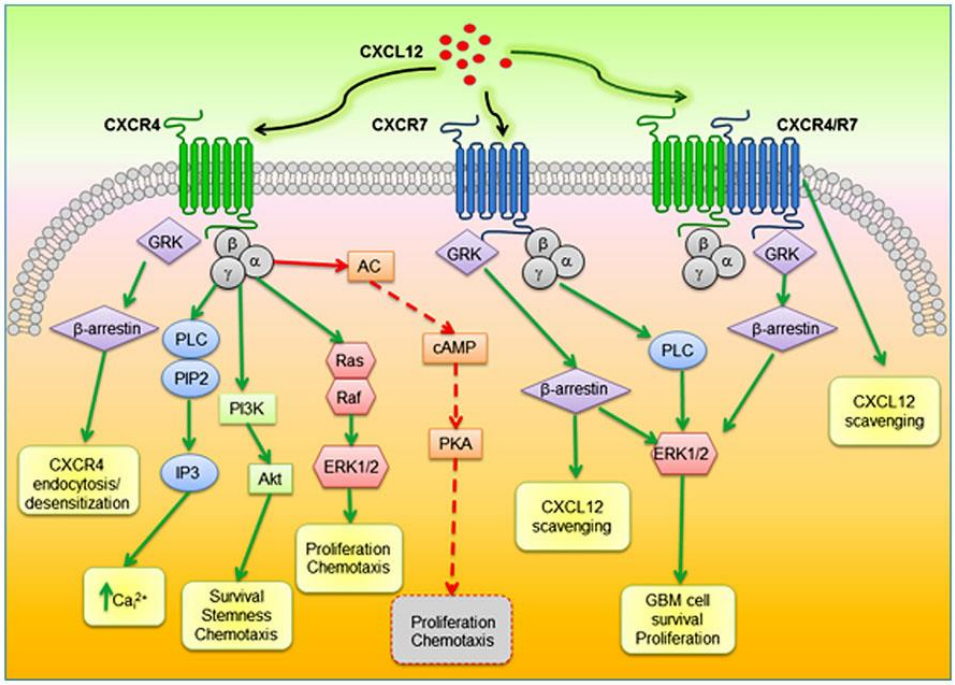

Figure 15 : CXCL12/CXCR4 and CXCL12/CXCR7 signalling pathways. CXCL12/CXCR4 pathway signalling lead to: (i) a rise in intracellular Ca^{2+} through PLC/IP3, (ii) chemotaxis, stemness, proliferation and survival features through PI3K/Akt, ERK1/2 and inhibition (red arrow) of AC mediated cAMP production, (iii) as well as CXCR4 internalisation through GRK/β-arrestin. CXCL12/CXCR7 pathway signalling lead to: (i) scavenging of CXCL12 through GRK/β-arrestin, (ii) as well as in survival and proliferation of GBM cells through PLC/ERK1/2. CXCR4/CXCR7 heterodimerisation changes CXCR4 G proteins conformation and blocks signalling.[43]

CXCL12 binding to CXCR4 results in GPCR signalling leading to: (i) a rapid and transient rise in the level of intracellular calcium ions through PLC/IP3, (ii) chemotaxis, stemness, proliferation and survival features through PI3K/Akt, ERK1/2, and inhibition of adenyl cyclase mediated cAMP production, (iii) as well as desensitisation (CXCR4 internalisation) through GRK/β-arrestin.[43] **(*Figure 15*)** In fact, it was suggested that low concentration of CXCL12 was positively correlated with migration, proliferation and differentiation. However, high concentration of CXCL12, such as concentrations observed in the SVZ and particularly around blood vessels, could promote quiescence.[44] The latter could be due to the previously mentioned desensitisation following internalisation of CXCR4 receptors at high CXCL12 concentrations.[44] This results in a down modulation of cell surface CXCR4 and thus a decrease of the effect of CXCL12 on $CXCR4^+$ cells.[47,48] Precisely, a rapid down modulation of CXCR4 was shown at concentration of CXCL12 over 125 nM (50% decrease in 5 min). These internalized receptors can subsequently recycle to the cell surface.[45]

Binding of CXCL12 to CXCR7 was also reported to have some effect on cell features especially in glioblastoma multiforme. Indeed, upon binding of CXCL12 to CXCR7, GPCR signalling results in: (i) scavenging of CXCL12 through GRK/β-arrestin, (ii) as well as in survival and proliferation of GBM cells through PLC/ERK1/2. Furthermore, CXCR4/CXCR7 heterodimerisation was reported to block CXCR4 signalling by inducing a conformational change of the receptor G proteins.[43] **(*Figure 15*)**

3.4. CXCL12/CXCR4 pathway in cancer and in glioblastoma multiforme in particular

3.4.1. Pathogenic role

The role of CXCR4/CXCL12 has been also reported in pathological conditions, as it showed to promote HIV entry, but in particular its function has been largely described in sustaining cancer progression.[19,41] Indeed, even though it is principally expressed by immune cells as said above, CXCR4 is also over-expressed on cancer cells. CXCR4 was shown to be related to various cancers and is considered as an unfavourable prognostic marker for renal or stomach cancer. The expression of CXCR4 and the production of CXCL12 inside tumours is, thus, considered as a hallmark of aggressiveness, especially of malignant glioblastoma. Indeed, CXCL12 and CXCR4 are aberrantly up-regulated in primary brain tumours like glioblastoma in comparison to the relatively low CXCL12 expression in normal adult brain tissue.[41] This high expression level of CXCR4 is usually correlated with poor prognosis for GBM patients.[19] Furthermore, it is positively correlated with tumours size and grade, and negatively correlated with patient survival. [19] Finally, this up-regulation is thought to promote tumour initialisation, as well as features like metastasis, angiogenesis and immunosuppression.[15,19,46,47] Some FDA approved drugs were developed to inhibit these pathogenic stimulations of CXCR4/CXCL12 signalling, such as AMD3100.[41]

3.4.2. GSCs in the pro-tumoral microenvironment

In GBM, CXCR4 and CXCL12 are mainly expressed or produced by GSCs, cancer associated fibroblasts (CAFs) and M2-like macrophages, but not by normal epithelial cells.[19] This expression increases with GBM grade. High levels of CXCL12 are observed in close proximity to degenerative zones and regions of tumour necrosis and angiogenesis. Besides, high expression of CXCR4 was localized in endothelial cells of neovessels.[41] Moreover, in hypoxic conditions, hypoxia inducible factors (HIFs, transcription factors) also increase CXCR4 expression in cancer cells, attracting endothelial progenitor cells (EPCs) for neoangiogenesis. CXCL12/CXCR4 pathway under hypoxia will also promote hypoxia adaptation of genes related to survival and migration.[19] Thus, CXCL12 and CXCR4 are expressed in GBM cells, upregulated in several conditions (mainly related to hypoxia and angiogenesis), and CXCL12/CXCR4 pathway can play several important roles.

First, CXCL12/CXCR4 pathway was demonstrated to promote proliferation in GBM cell lines and primary cultures. In CXCL12-producing $CXCR4^+$ GSCs, treatment with CXCL12 induced Akt-mediated survival and self-renewal as assessed by clonogenicity and neurosphere formation assays. This induction was inhibited by AMD3100, a CXCR4 antagonist, with a greater effect on cells producing high levels of CXCL12, indicating the importance of paracrine and autocrine loops.[46]

Secondly, CXCL12/CXCR4 pathway is involved in GSCs metastasis. GBM cells showed a CXCL12-dose dependent migration which could be inhibited by AMD3100. This migration behaviour was also suppressed in CXCR4 invalidated GBM cells both *in vitro* and *in vivo*. Finally, CXCR4/CXCL12 pathway was also shown to be involved in the migration of GSCs towards the SVZ.[1] Beside this direct effect on GSCs, CXCL12 also contributes to the microenvironment modification, by upregulating matrix metalloproteases (MMP2 and MMP9) leading to the ECM degradation which is an essential step in tumour metastasis, invasion and growth. MMPs are released by cancer cells at the apex of cytoskeletal protrusions called invadopodia formed by actin polymerization remodelling upon CXCR4 stimulation.[19]

The high expression of CXCL12 by endothelial cells close to regions of angiogenesis and the role of the CXCL12/CXCR4 axis in recruiting EPCs toward the tumour microenvironment to serve for neoangiogenesis were already mentioned above. In fact, CXCL12 produced by CAFs could also induce tumour cells to form vascular mimicry, which are channel-like structures used as alternative sources of nutrition and oxygen supply.[19] Furthermore, CXCL12 increases the production of the pro-angiogenic factor VEGF. This increase of production and microvessel density are both impaired by AMD3100 or CXCR4 knock-down. Binding of CXCL12 to CXCR4 might trigger VEGF production through the PI3K/AKT pathway by induction of Sp1 phosphorylation or by expression of several transcription factors such as HIF-1, in hypoxic condition.[11,37] VEGF will contribute to help GSCs in promoting angiogenesis via paracrine interactions between endothelial and tumour cells.[44] Note that a link between angiogenesis and stem cell self-renewal was pointed by the existence of proteins from the vascular niche (KIT ligand, PEDF, CXCL12, VEGF), which are involved in both processes.[44]

CXCR4/CXCL12 axis is also involved in immune modulation and suppression in several ways. First, CXCL12/CXCR4 pathway triggers the activation of inflammatory mediators such as NFκB which will regulate the expression of inflammatory cytokines in the tumour microenvironment. For example, this regulation was shown to reduce infiltration of cytotoxic T lymphocytes (CTLs) within the tumour. Secondly, CXCL12/CXCR4 axis is responsible for attracting mast cells (MCs), myeloid-derived suppressor cells (MDSCs), regulatory T cells (Tregs), and B cells to the tumour site. All these cells will supress normal anti-tumour immunity or impair CTLs activity. Last but not least, CXCL12/CXCR4 can induce cellular reprogramming. This is a particularly essential point as it can drive differentiation of monocytes or M1-like macrophages into pro-tumoral M2-like macrophages, which play a major role in controlling tumour progression in GBM microenvironment. Previously attracted neutrophils also undergo CXCL12/CXCR4-driven differentiation into a pro-tumoral N2 phenotype. In the same way, recruited mesenchymal stem cells (MSCs) will be transformed into CAFs able to reduce CTL infiltration in tumour microenvironment.[19]

In short, CXCL12/CXCR4 axis is involved in autocrine and paracrine stimulations within the tumour, participating in the creation of a specific pro-tumoral microenvironment at the tumour site.[1,12,19] This microenvironment will in turn promote self-renewal activity, metastasis of $CXCR4^+$ cancer cells and ECM remodelling, as well as tumour angiogenesis, immunosuppression, and cellular reprogramming.[19] This pathway is central in tumour growth and progression, and is correlated with tumour grade.[19] GBM therapies targeting this drastically central pathway seem therefore rather appropriate. **(*Figure 4*)**

3.4.3. GSCs/GICs in the SVZ niche

As mentioned previously, it was observed that GSCs, notably from human primary GB138 cells and human cell line U87MG cells, had the ability to escape the tumour mass in the striatum of immunodeficient mice tolerating xenografts and to migrate to SVZ environment, along the corpus callosum (CC), following a CXCL12 gradient.[1,47] In Boyden chamber assays, GBM cells isolated from the SVZ were shown to display a migration pattern much more influenced by CXCL12 concentration than those from the tumour mass.[1] In fact, the vessels covering the lateral wall of the ventricle are a major source of CXCL12 in the SVZ and major contributors in $CXCR4^+$ GSCs attraction. Indeed, it was shown that $CD133^+$ GSCs colocalise frequently with $CD31^+$ microvessel endothelial cells.[11,19]

The SVZ of the brain constitutes a specific niche sustaining the production of neurons and glial cells. It is a source of neuronal stem cells (NSCs) and neural progenitor cells (NPCs), essential for instance for the turnover of olfactory bulb interneurons.[44,48] The specific features of CXCL12/CXCR4 pathway described above contributes to the evolution of this neurogenic niche in a pre-metastatic niche for GSCs, in the GBM context. In this way, the SVZ niche maintains GSCs stem cell properties and protect them from standard therapies already mentioned (e.g. surgical resection, radiotherapy).[2,44] Furthermore, some studies demonstrated that a specific increase of SVZ irradiation significantly increase progression free and overall survival (PFS and OS) of GBM patients.[2,49] However, these data are still controlversial.[47,50]

As the SVZ microenvironment interacts with GSCs, it could play a dual role: one in tumour malignancy (precisely, metastasis and resistance to treatment), and the other in resurgence of GBMs tumours. On the one hand, as stated above, the SVZ constitutes a specific niche, notably containing chemoattractant (e.g. CXCL12) attracting NSCs or GSCs towards the neurogenic niche.[2,44] On the other hand, tumour recurrence could arise from GICs hidden in the SVZ during conventional treatment. These cells may migrate away from the niche to differentiate into a new more aggressive tumour, in a way similar to NPCs migrating towards surrounding injured regions.[44,47]

As a conclusion, in addition to reducing tumour growth and other features such as metastasis, angiogenesis and immunosuppression, GBM therapies targeting CXCL12/CXCR4 pathway could importantly reduce resurgence of tumours after standard therapies by disrupting GSCs/GICs abilities.

4. Metastasis, cell migration and epithelial-to-mesenchymal transition

4.1. Description

During this master thesis, we will focus on the impact of oHSV-P2G on the migration abilities of GSCs, in which the CXCL12/CXCR4 pathway seems to be involved.[1] Cell migration is an important aspect to investigate when studying the effect of a specific treatment on cancer. Indeed, migration is the basis of cancer metastasis as cancer cells need to migrate to escape the primary tumour site. Moreover, metastasis is a multi-stage process as cells need to survive during their circulation, seed at a distant organ-specific site of metastasis and, there, grow as a secondary tumour.[19] In the context of glioblastoma, metastasis allow resistance to standard treatments as GSCs migration towards the SVZ protect them from surgical resection. Disruption of metastasis mediated by oHSV-produced P2G is therefore a crucial aspect of the treatment.

The epithelial-to-mesenchymal transition (EMT) is a crucial feature of cancers related to metastasis as this process leads to the improvement of cell migration abilities.[51] EMT is a process whereby epithelial cells are transcriptionally reprogrammed in a way they lose their epithelial phenotype in favour of a mesenchymal one. This results in a switch from a polarized cell (phenotype characterized by specific cytoskeletal architecture, solid cell-cell junctions, and strong adhesion) to a mesenchymal phenotype with an increased ability to migrate, to degrade the extracellular matrix (ECM), and to invade surrounding or distant tissues (through the bloodstream and lymphatic system).[51–53] At the molecular level, these changes are marked by a switch from E-cadherin to N-cadherin expression, increased expression of mesenchymal vimentin, and upregulation of transcription factors like Snail, ZEB, and TWIST families.[51–53]

GSCs, as cancer stem cells (CSCs), could help in the formation of metastasis in sites distant from the primary tumour in the host by reversible EMT.[29,32] Indeed, following EMT-driven migration, the opposite process (MET) subsequently occurs and initiate tumour formation at the new site resulting in metastatic colonisation.[29,32] This consecutive switches between EMT and MET could be favoured by reversible epigenetic modifications and transcription factors that dynamically regulate features like cell adhesion.[51,52]

4.2. E-cadherin to N-adherin switch

The E-cadherin (120 kDa) to N-cadherin (130 kDa) switch is one of the earliest events in EMT either driving or resulting from the epithelial-to-mesenchymal transition.[26,29,33] Cadherins are type I transmembrane glycoproteins that mediate the calcium-dependent formation of adherent junctions between cells through interactions with other cadherin molecules.[56,57] It was observed that downregulation of E-cadherin, triggered by several inducers such as TGF-β, FGF, or NOTCH, leads to adherent cell-cell junctions breakdown, loss of cell polarity, and release of β-catenin involved in the WNT/β-catenin pathway further activating transcription factors.[51,56] These factors (e.g. SNAIL, SLUG, TWIST1/2, ZEB1/2) involved in cell proliferation and migration repress genes associated with epithelial phenotype, notably E-cadherin[29,30], and induce expression of mesenchymal phenotype-related genes such as fibronectin, N-cadherin and vimentin as well as matrix metalloproteases degrading the ECM like MMPs.[51] Besides, the Hedgehog (HH) signalling pathway, particularly SHH, also promotes EMT-mediated metastasis invasion by downregulating E-cadherin and increasing N-cadherin and vimentin production.[51] Finally, this cadherin switch leads to a motile phenotype also thanks to increased expression of RAC, Cdc42, and RhoA that promotes cytoskeleton rearangment.[26]

Thus, in most cases, E-cadherin decrease is described as a feature of aggressive tumours and is correlated with EMT-driven invasion of metastatic cancers.[26,33] On the molecular level, transmembrane E-cadherins interactions inhibits Wnt/β-catenin and PI3K pathways preventing EMT.[26] However, high-level of E-cadherin expression were shown to increase tumour progression in some cancers including glioblastoma.[26] This dual role could be explained by the existence of a soluble E-cadherin (80 kDa) resulting from cleavage of the transmembrane one.[26] This soluble form is produced following the EMT and interferes with adherens junctions, increasing cancer cell migration through MMPs production and signalling pathways activation.[26]

N-cadherin is less prevalent in non-epithelial tissues and more in neural and endothelial cells. N-cadherin increase is correlated with EMT.[26] On the molecular level, N-cadherin-mediated adherens junction activate MAPK/ERK, STAT3, and PI3K pathways leading to enhanced survival and migration.[26] Related to GBM, N-cadherin signalling was demonstrated to significantly enhanced polarity and, thus, directional migration of NPCs from the SVZ to lesion sites.[58] Nevertheless, it was shown in some cases that N-cadherin could establish strong adherens junctions in the neural crest cells, inhibiting EMT, and its downregulation promoted metastasis in neuroblastoma.[26]

4.3. Migration and vimentin

Several intermediate filaments proteins (IFP), which are the third main component of the cytoskeleton, play an important role in cell migration and contraction.[59,60] Beside cadherins, vimentin is also often used as a cell migration and EMT marker.[36,37]

It has been shown that vimentin expression level could be associated with the ability of cells to migrate.[36,37] Moreover, the most migrating cells in human adults are leukocytes and fibroblasts, and vimentin is the principal IFP expressed in those cells.[59] Finally, malignant tumours helped to demonstrate that there was a correlation between vimentin expression and cancer cells migration/invasion in surrounding tissues.[59] Indeed, vimentin level was upregulated in high-grade and highly invasive gliomas.[37] Interestingly, a signalling pathway leading to vimentin upregulation included ZEB2 as transcription factor which was shown above to be involved in EMT-driven migration phenotype.[29,30,37]

Precisely, it was suggested that vimentin does not directly increase cell migration but enhance its directionality. This leads to an improved effectiveness of migration abilities by polarizing the cells and thus, increasing the duration of the motion in a specific direction.[59]

4.4. Strategy

During this master thesis, the effect of P2G on migration will be evaluated by using P2G-containing media (conditioned media) derived from infection by oHSV-P2G of monolayers of GB138 cells for 48h in DMEM media without growth factors. This media will be centrifuged and filtered (0.1 µm) to remove cell membrane debris and viral particles. Media derived from 48h of culture of GB138 cells uninfected or infected by not-armed oHSV will be used as control. For these experiments, human primary cells growing only as 3D neurospheres *in vitro* will be used (T08, T013), as well as human (GB138) primary cells and murine (GL261 N^+) cell lines growing as 2D monolayers. Migration phenotype will be analysed *in vitro* on the 3D models and migration markers (vimentin and cadherins) expression will be investigated. In parallel, the invasion abilities of GB138 and GL261 N^+ cells will be assessed. This will allow us to show the impact of oHSV-P2G treatment on CXCL12/CXCR4-promoted migration abilities of GBM cells, which are mainly related to the presence of GSCs. AMD3100, FDA-approved CXCR4/CXCL12 inhibitor, will be used as a control showing the impact of interfering with CXCR4/CXCL12 pathway.

II. Materials

1. Antibodies

The different antibodies are listed in Appendices. **(*Table 1*)**

2. Buffers

2.1. Agarose Gel Electrophoresis (AGE)

2.1.1. Tris-Acetate-EDTA (TAE)

Buffer used to limit heating related to Joule effect during DNA migration in AGE. This buffer consists of: 40 mM Tris-Acetate ; 1 mM EDTA ; pH 8.

2.2. Bacmid Maxipreparation

2.2.1. P1 buffer

Bacteria resuspension buffer used for maxipreparation. This buffer consists of: 50 mM Tris ; 10 mM EDTA ; 100 µg/mL RNase ; pH 8.

2.2.2. P2 buffer

Bacteria lysis buffer used for maxipreparation. This buffer consists of: 200 mM NaOH ; 1% SDS.

2.2.3. P3 buffer

Buffer used to neutralize the alkaline lysis and precipitate proteins during maxipreparation. This buffer consists of: 3 M potassium acetate ; pH 5.5.

2.3. Immunofluorescence

2.3.1. Phosphate Buffer Saline - Triton® X-100 (PBS-T)

Buffer used for membrane permeabilization before immunolabeling and nuclei staining. This buffer consists of 0.2% triton diluted in PBS.

2.4. Western Blotting

2.4.1. Loading buffer

Buffer used to load the proteins into the wells of the polyacrylamide gel. This buffer consists of: 10 mM Tris ; 1% SDS ; 25% glycerol ; 0.1 mM β-mercaptoethanol ; 0.03% bromophenol blue.

2.4.2. Migration buffer

Buffer used for protein migration during PAGE. This buffer consists of: 50 mM Tris ; 192 mM glycine ; 3.5 mM SDS.

2.4.3. RIPA lysis buffer

Buffer used to induce cell lysis and obtain a total protein extract in solution after centrifugation. This buffer consist of: 50 mM Tris-HCl pH 7.5 ; 1 mM EDTA ; 150 mM NaCl ; 0.25% sodium deoxycholate ; 1% NP40 (Roche) ; 2% proteases inhibitor 50x complete (Roche).

2.4.4. Transfer buffer

Buffer used for protein transfer from the polyacrylamide gel to the polyvinylidene fluoride membrane (PVDF ; GE Healthcare). This buffer consists of 25 mM Tris ; 192 mM glycine ; 20% methanol.

2.4.5. Tris-Buffered Saline Tween (TBS-T)

Buffer used to wash away excess antibodies from PVDF membranes. This buffer consists of: 20 mM Tris-HCl pH 7.6 ; 150 mM NaCl ; 5% Tween (VWR Chemicals).

2.5. Various assays

2.5.1. Phosphate Buffer Saline (PBS)

Buffer used as not toxic for cells, consisting of: 137 mM NaCl ; 2.7 mM KCl ; 10 mM Na_2PO_4 ; 1.8 mM KH_2PO_4 ; pH 7.4.

3. Cell lines

Cell lines are cultured in DMEM HG 10% FBS (2D primary cells and VERO cells) or in neurosphere media (3D primary cells) and incubated at 37°C with 5% CO2.

3.1. 2D cell lines

These cells are cultured as 2D monolayers and used for conditioned media production (GB138) and for laminin-coated transwell invasion assay (GB138, GL261 N+). These cells can also be grown as 3D neurospheres if cultured in neurosphere media.

3.1.1. GB138

GB138 cells are human GBM tumour mass primary cells.

3.1.2. GL261 Nectin$^+$ (GL261 N$^+$)

GL261 N+ cells are murine GBM tumour mass cells from a commercial cell line. They were transduced with the human nectin to make them more susceptible to HSV-1 infection.

3.2. 3D primary cell lines

Conversely to 2D cell lines, these 3D primary cells are cultured as 3D neurospheres/spheroids in a specific neurosphere media. These cells are used for spheroid migration assays and for analysis of migration markers expression.

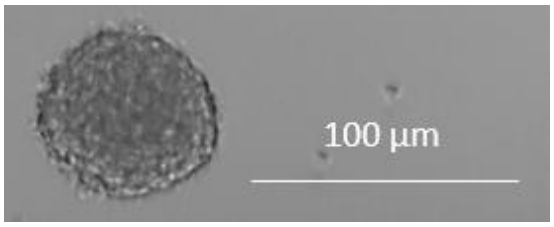

Figure 16 : T013 3D Neurosphere. T013 GBM primary cells under a microscope grown as neurosphere.

3.2.1. T08 cells

These cells are GBM tumour mass primary cells showing low expression of CXCR4 at the cell membrane and are thus used as a negative control for P2G effect on cell migration and migration markers.

3.2.2. T013 cells (*Figure 16*)

These cells are GBM tumour mass primary cells showing a higher expression of CXCR4 at the cell membrane than T08 cells and are thus used to assess P2G effect on cell migration and migration markers.

3.3. VERO cells

VERO cells are adherent epithelial cells derived from monkey's kidney (*Cercopithecus aethiops*). This cell line is permissive and susceptible to many viral strains, notably HSV-1, and is used for the production of high quantities of viruses and for virus titration.

4. Media

4.1. Bacterial cell culture

4.1.1. Lysogeny broth (LB) media

This media is used for bacterial cell culture and consists of: 10 g/L tryptone ; 5g/L yeast extract ; 10 g/L NaCl.

4.2. Mammalian cell culture

4.2.1. Dulbecco's Modified Eagle Medium/F-12

DMEM/F-12 without growth factors media is used in the production of neurosphere media as well as in the production of conditioned media, and to dilute the latter in migration and invasion experiments.

4.2.2. Dulbecco's Modified Eagle Medium High Glucose (Lonza) 10% FBS

DMEM HG media complemented with 10% Foetal Bovine Serum (FBS, Gibco®) is used for culture of 2D cell lines and VERO cells.

4.2.3. Neurosphere media

This media is used for the culture of 3D primary cells and consists of DMEM/F-12 without growth factors complemented with B-27™ supplement without vitamin A (50X) 1:50, heparin 1µg/mL, hFGF 20 ng/mL, EGF 20 ng/mL.

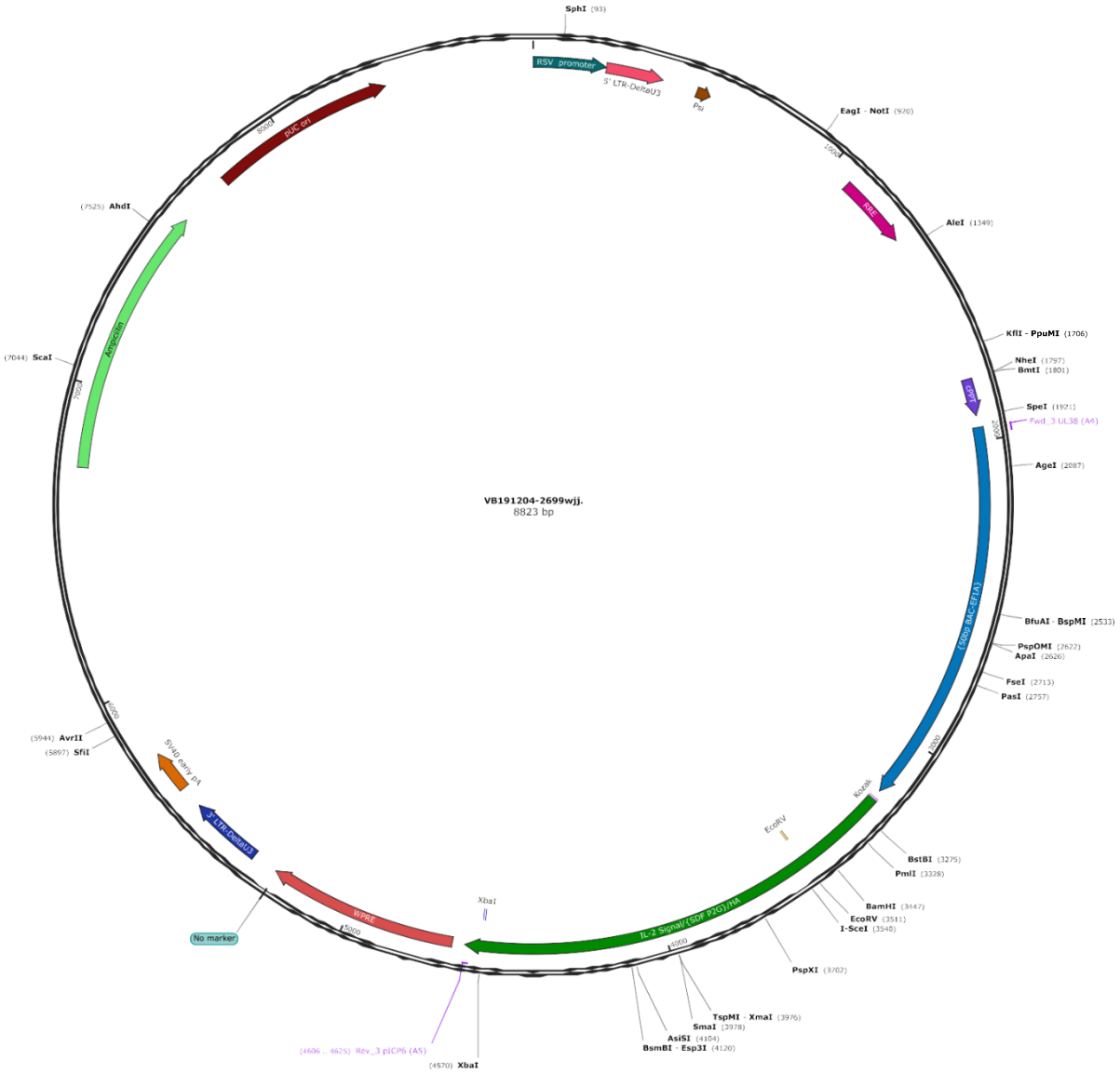

Figure 17 : pEF1a-P2G plasmid map (VB191204-2699wjj.). *Schematic representation of pEF1a-P2G plasmid generated on SnapGene Viewer.*

4.3. Virus production and titration

4.3.1. Virus production-serum free medium (VP-SFM, Gibco)

This media a serum-free with ultra-low protein concentration (5 µg/mL) designed for the growth of VERO cells for virus production used for the production of high quantities of virus before its purification by ultracentrifugation.

4.3.2. Methylcellulose media overlay

This media is used to prevent viruses to spread and generate foci to sites distant from primary infection during a titration by pfu assay. This media consists of: 3 g/L methylcellulose ; 1:5 PBS ; 4:5 DMEM HG 10% FBS.

5. Oligonucleotides

Oligonucleotides sequences are listed in Appendices. **(*Table 2*)**

6. Plasmids

The insertion cassette used for by-passing cloning of oHSV-P2G is contained in a plasmid (pEF1a-P2G plasmid, VB191204-2699wjj.) including notably the gene for P2G expression under the control of the strong mammalian promoter pEF1a. **(*Figure 17*)**

7. Polyacrylamide gel

Polyacrylamide concentration for the concentration and separation gel are of 4% and 13%, respectively. Gel composition is described in Appendices. **(*Table 3*)**

8. Viruses

oHSV are derived from the Herpes Simplex Virus 1 F strain (fHSV-1) with deletion of ICP34.5, ICP6, ICP47 (oHSV ΔICP34.5 ΔICP6 ΔICP47), and expressing Green Fluorescent Protein (GFP) under control of a CMV-derived immediate early (IE) promoter (fQuik1). Viral genomes are contained in bacterial artificial chromosomes (BACs) to facilitate cloning. Viruses used are described in Appendices. **(*Table 4*)**

III Methods

1. Agarose gel electrophoresis (AGE)

The aim of AGE is to induce separation of DNA molecules according to their size and conformation through the use of a tension generating an electric field. Shorter DNA molecules migrate faster than longer ones as they move more easily through gel pores.

Preparation of 1% agarose (Eurogentec) gel was done with 0.5xTAE and Midori Green (Filter Service) 1:10000. A slot is loaded with a DNA marker, namely Gene Ruler DNA Ladder Mix (Thermo Scientific). A voltage of 90 V was applied for 15 min of migration.

2. Agarose gel extraction

The aim of agarose gel extraction is to retrieve and purify a specific DNA molecule, previously separated by AGE. This extraction was done following the NucleoSpin® Gel and PCR Clean-up kit (Machery-Nagel).

3. Bacmid maxipreparation

A selected clone is inoculated in 500 mL of LB media + 12.5 µg/mL chloramphenicol and the pre-culture is incubated ON at 32°C. After incubation, a pellet is obtained by centrifugating 10 min at 6000 rpm (3381 g) 4°C. The pellet is then resuspended in 50 mL of P1 buffer. 50 mL of P2 buffer are added and gently homogenized before 5 min incubation at RT. 50 mL P3 buffer are added and the tubes are mixed until a white floating deposit appears. After 15 min of incubation on ice, the tubes are centrifugated for 15 min at 6000 rpm and the supernatant is filtered using a compress. Followingly, nucleic acids are precipitated by adding 100 mL of isopropanol before being pelleted by 10 min of centrifugation at 8000 rpm (6010 g). The supernatant is discarded and the pellet is dried for 5-10 min.

At this stage, some RNA residues are still present and must be eliminated. For this reason, the pellet is resuspended in 10 mL ammonium acetate 2M and incubated on ice for 1h before being centrifugated 10 min at 8000 rpm. The supernatant is transferred to a 35 mL tube and DNA is again precipitated by adding 7 mL isopropanol (ice-cold) before being pelleted by 10 min of centrifugation at 8000 rpm. The supernatant is discarded and the pellet is dried for 15 min.

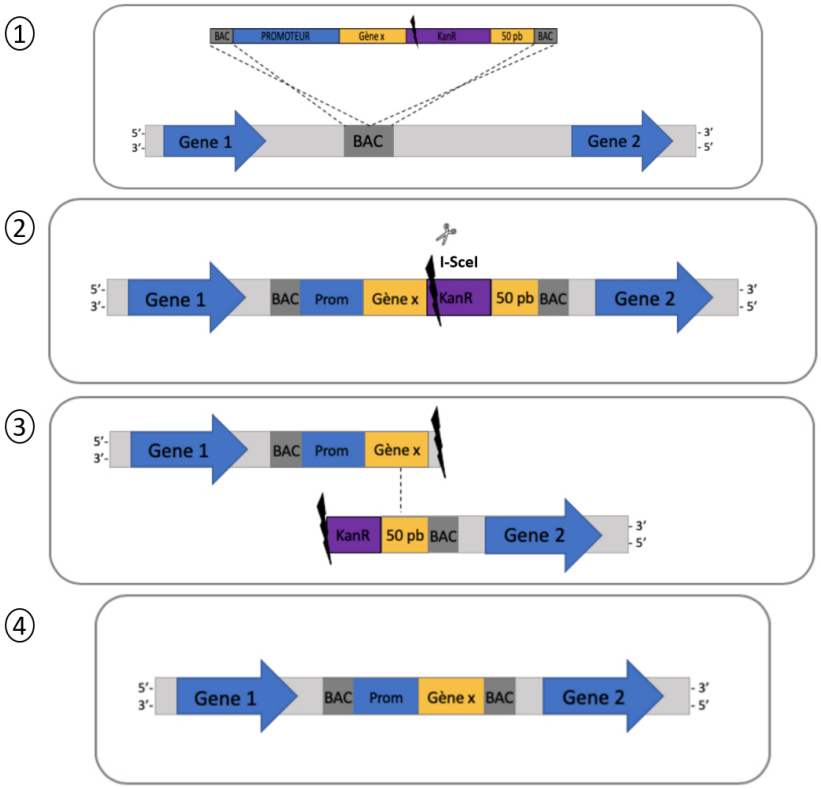

Figure 18 : By-passing cloning.. Schematic representation of by-passing cloning experiment with 1) first Red recombination, 2) I-SceI induction and restriction into kanR sequence, 3) second Red recombination, and 4) final result of by-passing cloning.

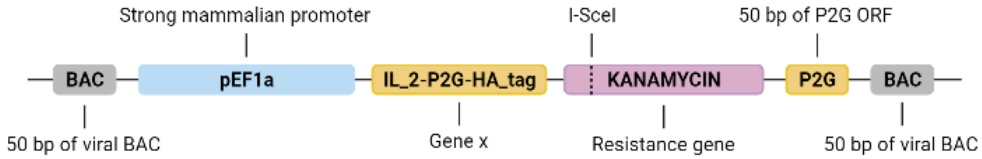

Figure 19 : pEF1a-P2G insertion cassette. Schematic representation of the insertion cassette used to create oHSV-P2G from oHSV by by-passing cloning. Inserted gene x contains P2G ORF preceded by IL-2 signal peptide and followed by HA-tag. *Created with BioRender.com*

The last step consists in DNA purification on a caesium chloride gradient. The dried pellet is resuspended in 4 mL of TE buffer (Tris 10 mM pH 7.5 ; EDTA 1 mM). The solution is transferred in a 50 mL tube, 4g of caesium chloride and 400 µL of ethidium bromide (10 mg/mL) are added before 15 min of centrifugation at 4°C and 3000 rpm (845 g). Subsequently, the clarified solution is transferred into an ultracentrifugation tube for VTi 65.2 rotor and centrifugated for 16-18h at 45000 rpm (169419,6-199357,2 g), 4°C. Two bands appear and are separated in two tubes. Ethidium bromide is eliminated by 5 successive extraction with isoamyl alcohol (V/V). The phase containing the DNA is transferred into a 35 mL tube, 3 volumes of water, and 8 volumes of ethanol absolute (ice-cold) are added to precipitate DNA. A pellet is formed by centrifugation (10' - 8000 rpm), washed with 5 mL of ethanol 70%, centrifugated again (15' - 8000 rpm), and dried for 30 min at RT. Finally, the pellet is dissolved in 200 µL of Tris 10 mM pH 8.

4. By-passing cloning[61] (***Figure 18***)

The by-passing cloning technique allow the modification (addition, deletion or mutation of genes) of oHSV genome encoded in a BAC using a insertion cassette with a bifunctional marker **(*Figure 19*)** and a recombinogenic bacterial strain (*E. Coli* GS1783). This technique includes a first recombination allowing the selection of clones which integrated the insertion cassette in their BAC thanks to a selection marker granting resistance to kanamycin. Subsequently, a second recombination removes this selection marker from the BAC. Thus, several characteristics of the insertion cassette and the bacterial strain are important. (i) The ends of the insertion cassette must be homologous to a specific region of the BAC. (ii) The cassette must contain the sequence of interest to insert and a 50 bp complementary region for this sequence separated by a kanR selection marker with a *I-SceI* restriction site. (iii) The recombinogenic bacterial strain must contain inside its genome the recombination system of the λ phage, namely *exo*, *bet*, and *gam* genes. These genes are under control of a temperature-sensitive repressor (*c1857*), thus, they are not expressed when bacteria are incubated at 32°C. The gene *exo* codes for a 5'-3' exonuclease which induces the formation of cohesive ends at the extremities of the insertion cassette. The *bet* gene codes for a recombinase which favours homologous recombination with the BAC by binding to those ends. The *gam* gene codes for an inhibitor of *E. Coli*'s exonucleases to avoid degradation of the insertion cassette.

4.1. PCR amplification of the insertion cassette

The insertion cassette is amplified from a plasmid by PCR. Subsequently, the PCR product is incubated for 90 min with 1 µL of DpnI. This restriction enzyme hydrolyses the plasmid template but not the PCR product as it recognizes only methylated bacterial DNA. An AGE is performed and the amplified insertion cassette is extracted from the gel and purified.

4.2. First Red recombination

Before transforming bacteria with the purified PCR product, *E. Coli* GS1783 cells containing the BAC of interest must be made electrocompetent. A pre-culture of 5 mL of LB media with 12.5 µg/mL of chloramphenicol (Cm) to maintain the BAC is incubated ON at 32°C with agitation (220 rpm, using Eppendorf / New Brunswick Scientific C25 Incubated Floor Model Shaker). The next day, 5-200 mL of LB media + Cm are inoculated with the pre-culture (1:20 or 1:50) and incubated at 32°C under agitation until the optical density at 600 nm (DO_{600}) reaches 0.5-0.7.

GS1783 are made electrocompetent by thermal shock in a water bath shaker (15' - 42°C - 220 rpm ; 4°C/ice - 20 min). The culture tube is centrifugated for 5 min at 4500 g, 4°C. The supernatant is discarded and the bacteria are washed 2-3 times with ice-cold 10% glycerol. The pellet is finally gently resuspended in glycerol 10% (1:100 of culture volume). For electroporation, freshly prepared bacteria can be used as well as frozen down bacteria in aliquots in a dry ice/ethanol bath and stored at -80°C.

For electroporation, 100 ng of PCR product are used in 100 µL bacteria with the following settings: 17.5 kV/cm (1.75 kV with 0.1 cm cuvettes), 25 µF, and 200 Ω. Bacteria are transferred to 1 mL LB without antibiotics and incubated at 32°C for 1h under agitation. Plate 100 µL and 700 µL on LB + 12.5 µg/mL chloramphenicol + 25 µg/mL kanamycin and incubate at 32°C for approximately 24h-48h. 10-15 candidate clones are analysed by colony PCR and the products are separated by AGE to confirm presence or absence of the insertion cassette.

4.3. Second Red recombination

Selected clones from the previous step are added to a pre-culture and incubated ON at 32°C in 5 mL LB media + 12.5 µg/mL chloramphenicol + 25 µg/mL kanamycin under agitation. The next day, inoculate with 250 µL of fresh ON culture to the 5 mL of LB media + 12.5 µg/mL chloramphenicol but without kanamycin. Grow culture for 1h30-2h at 32°C under agitation until the DO_{600} reaches 0.4-0.5 (early logarithmic phase). Remove excessive culture to keep only 2 ml in the tube. Add 2 mL of warm LB media + Cm + 1% arabinose and incubate under agitation for 50 min at 32°C (induction of I-SceI expression). The culture is transferred into a 42°C water bath shaker (220 rpm) for exactly 15 min (c1857 repressor expression supressed, induction of expression of Red recombination system). The culture is put back to 32°C for 3h. Finally, two dilutions (100 µL of 10^{-5} and 10^{-6}) are plated on agar plates with LB + Cm + 1% arabinose and incubated for 24-48h. 10-15 candidate clones are analysed by colony PCR and the products are separated by AGE to confirm for correct recombination and deletion of the selection marker kanR. Selected clones are send to sequencing to check for single mutations and inoculated on agar plates LB + Cm + Kana to confirm absence of kanR.

5. Conditioned media production

The aim of this experiment is to produce important quantities of media derived from cells infected by oHSV-P2G GB138 infected cells. This media will be used to assess the effect of P2G produced upon infection on cell migration. Media derived from uninfected cells or cells infected by oHSV will be used as control.

GB138 cells are grown in p175 flasks with 20 mL DMEM HG 10% FBS. When cells reach confluence, media is replaced by DMEM without growth factors (growth factors have a negative impact on migration on their own) with an infection at MOI of 1. After 48h, media is collected in 50 mL Falcon, centrifugated to remove cellular debris, and the supernatant is filtered with 0.1 µm filter to remove viral particles. The filtered media is then stored at -80°C in aliquots of 1 mL.

6. Enzyme-linked immunosorbent assay (ELISA)

The aim of this experiment is to determine the concentration of a specific protein in a solution (here, P2G detected thanks to its coupled HA-tag in conditioned media). The ELISA is realised following the human HA tag ELISA KIT (MyBioSource).

7. Immunofluorescence (IF)

The aim of this experiment to use antibodies labelled with fluorescent dyes to demonstrate the presence of a particular antigen in a tissue preparation. Migrating neurospheres in a 96-well plate coated with poly-D-lysine, derived from the spheroid migration assay, are fixed with PFA 4% during 10 min at RT. Then, cells are washed 3 times with PBS before being incubated 5 min with PBS-T 0.2%. Afterwards, the wells are again washed 3 times with PBS and incubated for 1h with BSA 2% for blocking. Subsequently, the cells are incubated ON at 4°C with the primary antibody diluted 1:200 in PBS-T 0.2% BSA 2%. In the dark, the cells are washed 3 times with PBS before adding the secondary antibody coupled to a fluorescent dye diluted 1:500 in PBS-T 0.2% BSA 2% for 1h and, following washes, Hoechst for 5 min. The cells are finally washed and maintained at 4°C until imaging with the Nikon A1R Confocal Microscope. Pictures are analysed by ImageJ to assess the intensity of fluorescence signal.

8. Laminin-coated transwell invasion assay

The aim of this experiment is to assess the invasion ability of specific cell lines through the ECM. ThinCerts™ transwell (greiner bio-one, cellstar®) with 8 µm of pore size are placed in a 24-well plate. (greiner bio-one). The upper chamber, inside of the insert, is filed with 60 µL of 0.02 mg/mL laminin and put to incubate for 24h at 37°C. Subsequently, the excess laminin is removed and the adequate number of cells (25k for GL261 and 20k for GB138) is added in the upper chamber in DMEM culture media without growth factors and conditioned media 50:50 for a final volume of 200 µL. The cells are left to migrate for 48h at 37°C attracted by 300 µL DMEM High Glucose media containing 10% FBS in the lower chamber.

After two days, media and cells in both chambers are removed, the inserts are washed with PBS and cells are fixed with PAF 4% for 10 min. The transwells are washed again with PBS, before being immersed in crystal violet for 10 min. Exceeding dye is washed several times with PBS and remaining non migrating cells in the upper chamber are removed using a cotton swab. chamber of a 24-well plate. The number of cells passing through the laminin coating are counted. The % of invading cells is measured as $\frac{Number\ of\ invading\ cells}{Number\ of\ plated\ cells} * 100$.

9. Polymerase chain reaction (PCR)

The aim of this experiment is to amplify a specific region of DNA. A mix is prepared containing 1 µL of template, 10µM of primers specific for the amplified region, 10 mM of dNTPs, reaction buffer with MgCl2 (Promega) and the enzyme Go Taq® G2 Polymerase (Promega). For PCR, the thermocycler (Mastercycler® Pro - Eppendorf) parameters are as follow: 1) initial denaturation (5’ - 94°C), 2) 35 cycles (denaturation, 30’’ - 94°C ; hybridization, 30’’ - 58°C ; elongation, x - 72°C), 3) final elongation (2’ - 72°C). The elongation time during the cycles depend on the size of the amplified region (1min/kb for Go Taq® G2 Polymerase synthesis). The PCR products are further analysed by AGE.

10. Reverse transcription-quantitative PCR (RT-qPCR)

The aim of this experiment is to assess the relative quantity of a specific RNA molecule in order to determine the level of expression of a specific gene. Total RNA extracts are obtained from cell pellets following the NucleoSpin® RNA kit (Machery-Nagel) and concentration is measured using nanodrop (Thermo Scientific®). Subsequently, reverse transcription is performed to convert RNA into complementary cDNA following the RevertAid H Minus First Strand cDNA Synthesis kit (Thermo Scientific®). Then, a mix is prepared containing 20 ng of cDNA, 0.2 µM of primers specific for the targeted mRNA, 10 µL of SYBR green (Takyon – Eurogentec), complemented to 20 µL with nuclease-free water (Cytiva HyClone™). For qPCR, the thermocycler (LightCycler® 480 Real-Time PCR System – Roche) parameters are as follow: 1) enzyme activation (3' - 95°C), 2) 45 cycles (5'' - 95°C ; 30'' - 60°C with single acquisition), 3) melting curve (10'' - 95°C ; 10'' - 60 °C ; 95°C with continuous acquisition), 4) cooling (10'' - 40°C). The relative quantity of mRNA in each samples is further calculated based on the crossing points (Cp, cycle at which fluorescence from amplification exceeds the background fluorescence) given by the thermocycler.

11. Spheroid migration assay

Wells of a 96-well plate are coated with 50 µL of 10 µg/mL poly-D-lysine hydrobromide during 30 min. The wells are then washed with sterile water and left to dry under the hood overnight. Neurospheres are plated in DMEM media without grow factors + conditioned media derived from infected cells 50:50. After 1 hours of incubation, pictures of fixed neurospheres are taken with optical microscope. After 36 hours of incubation, pictures of the migrating cells are taken by optical microscope. The migration level is measured using ImageJ as follow: $\% \, of \; migrating \; area = \frac{Area \; 48h - Area \; 1h}{Area \; 48h} * 100.$

12. Titration

The aim of this experiment is to quantify the concentration of infectious viral particles in an aliquot. 160 000 VERO cells are plated in 18 wells of a 24-well plate in DMEM HG media. The following day, the media is replaced by 185 µL of DMEM media without growth factors containing one of 6 different dilutions, each in triplicates (10^{-5} ; $2.5x10^{-6}$; 10^{-6} ; $2.5x10^{-7}$; 10^{-7} ; $2.5x10^{-8}$). After 1h30 of incubation at 37°C, the infection media is replaced by 1 mL fresh media containing methylcellulose and incubated at 37°C for 48h. Subsequently, cells are fixed with 200 µL of PAF 4% during 20 min before replacing it with 500 µL of PBS. The infection foci are observed using the IncuCyte® and the concentration is measured in plaque forming unit per volume: $\frac{\mathrm{PFU}}{\mu L} = \frac{Mean \; number \; of \; foci/well}{Dilution \; x \; Infection \; volume}$.

13. Transfection

The aim of this technique is to insert the recombinant BAC, containing the viral genome, in mammalian cells able to produce infectious viral particles. In a first tube, 6 µg of purified DNA are mixed with 100 µL of NaCl 150 mM. In a second tube, 6 µL of Jet PEI (Polypus) are also diluted in 100 µL of NaCl 150 mM. The latter solution is added to the first one and incubated for 15 min at RT. The 200 µL of solution are then transferred to recently defreezed VERO cells in a 6-well plate at 40% confluence ($4.8x10^5$ cells/well).

14. Virus purification by ultracentrifugation

The aim of this experiment is to produce a highly concentrated (pfu/µL) virus stock that can be used both *in vitro* and *in vivo*. 12 p175 flasks are seeded with VERO cells at 80-100% confluence in DMEM HG 10% FBS (100% confluence corresponds to $1.8x10^7$ cells in a p175 flask). Then, media is replaced by 7 mL VP-SFM media without FBS added with virus at a MOI of 0.005. Cells are incubated with the infection media at 37°C for 90 min with rocking plate every 15 min to ensure the inoculum covers the entire monolayer. The volume of VP-SFM media is then elevated to 20 mL for 24h of incubation at 37°C. The infection is finally continued for 4 additional days at 33°C.

Subsequently, the infection media is added with NaCl and dextran sulphate at a final concentration of 0.045 M and 100 µg/mL, respectively, and incubated again ON at 33°C. The flasks are transferred at RT on a rocking plate for 90 min to completely detach all cells from the monolayer. Media and cells can now be collected in six 50 mL tube and centrifugated at 4°C, 2200 g for 10 min to spin down cell debris. The supernatant is filtered with 0.8 µm filter before pelleting the virus using high-speed centrifugation (41657-47850 g) 17000 rpm for 1h at 4°C. Supernatant is removed and the pellet is washed with PBS to remove residual salt and dried. Then, the pellet is resuspended by covering the visible pellet with 50 µL PBS ON at 4°C. Add glycerol to a final concentration of 10%, mix, and aliquot in 1.5 mL Eppendorf. Store at -80°C.

15. Western Blotting (WB)

The aim of WB is to detect small quantities of proteins thanks to target-specific antibodies after separation according to their size via Polyacrylamide Gel Electrophoresis (PAGE). Cell pellets were lysed for 30 min on ice with RIPA buffer. The total protein extract is then centrifugated at 4°C, 12000 rpm (13523 g) for 20 min and protein concentration is measured using the Bradford (Biorad) method with BSA (Fisher Scientific) as a protein quantitative standard. Loading buffer is added to 50-80 µg of proteins which are incubated for 5 min at 95°C. Subsequently, the proteins are separated by PAGE in migration buffer, before being transferred onto a PVDF membrane activated by methanol (GE Healthcare) in transfer buffer. Then, the membrane is sealed by TBS-T milk 5% for 30 min, added with mouse or rabbit primary antibodies 1:1000, and incubated overnight at 4°C. The next day, the membrane is washed by TBS-T for 3 times 5 min. Followingly, it was incubated for 1h in TBS-T milk 1% with HRP-linked goat anti-rabbit or horse anti-mouse secondary antibody 1:2500 (Cell Signalling Technology®). The membrane is again washed by TBS-T for 3 times 5 min. Finally, electro-chemiluminescence (ECL) is used to detect the hybridization signal with ImageQuant LAS4000 (GE Healthcare).

16. Statistical analysis

Data are expressed as mean + SEM. Two-tailed paired student t test were used as 2 groups were always compared (GraphPad Prism 8.0.1.). All presented experiments were done in triplicates (n=3). P-value < 0.05 (*) are considered statistically significant.

CXCR4 expression in different cell lines

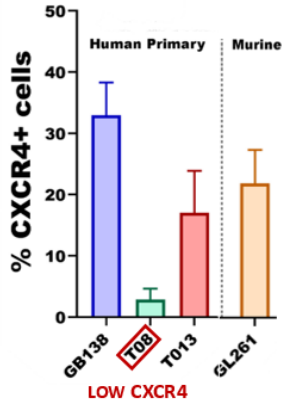

Figure 20 : CXCR4 expression in different cell lines. FACS analysis of CXCR4 expression in different human (GB138, T08, T013) and murine (GL261) GBM cell lines. (Paolo D'Arrigo, post-doc)

Spheroid assay for different cell lines

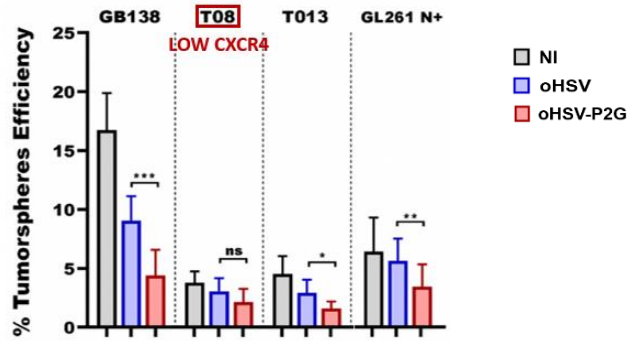

Figure 21 : Spheroid assay in different cell lines. Spheroid assay in different human (GB138, T08, T013) and murine (GL261) GBM cell lines infected with oHSV and oHSV-P2G (Paolo D'Arrigo, post-doc)

IV. Results

1. Preliminary results

1.1. CXCR4 expression in different cell lines

Some preliminary results, obtained by Paolo d'Arrigo (post-doc), essentially had to be collected before analysing the effect of P2G-containing media on GBM cells migration, invasion and metastasis. The most important one is maybe the analysis of CXCR4 expression by the cell lines used in the laboratory. The production of CXCL12 by these cell lines is also important to investigate as it is responsible for the mechanism that P2G treatment is supposed block.

FACS analysis revealed a significantly lower proportion of CXCR4 positive cells among T08 cells. The three other used cell lines (T013, GB138, GL261) conversely showed between ~15% to ~30% of CXCR4 positive cells in culture. **(*Figure 20*)** Furthermore, the production of CXCL12 for each cell line was shown to be correlated to CXCR4 expression. **(*Data not shown*)** Besides, the percentage of $CXCR4^+$ cells and the production of CXCL12 increased in cells cultured in 3D compared to cells cultured in 2D. **(*Data not shown*)**

As the treatment is supposed to affect the CXCL12/CXCR4 pathway, cells which do not express CXCR4 should not be impacted. Therefore, T08 cells were considered as a potent negative control for treatment efficiency.

1.2. Impact of oHSV-P2G on GBM cells stem-like features

Other preliminary results (spheroid, clonogenic, and stem markers expression assays) demonstrated the potential of oHSV-P2G to impair CXCL12/CXC4 pathway and the ability of the treatment to decrease the presence of GSCs (decrease in GBM stem-like features). These results are interesting as they are direct consequences of the decreasing of GSCs presence, which will further result in a decrease of GBM cells CXCL12/CXCR4-driven migration abilities.

First, the spheroid assay evaluates the self-renewal abilities of GBM cells growing in 3D by measuring tumorosphere formation efficiency, which consists in the ability of GBM cells to form neurospheres in culture. For this assay, different cell lines previously infected for 18h with oHSV or oHSV-P2G were plated at a specific density depending on the cell line. After 7 days, the percentage of tumorosphere formation efficiency is measured as $\frac{\text{Number of tumorospheres}}{\text{Number of plated cells}} * 100$. This assay successfully showed a significant decrease in tumorosphere formation efficiency for GB138, T013, and GL261 N+ cells infected with oHSV-P2G compared to oHSV infected cells. Conversely, T08 cells (low proportion of $CXCR4^+$ cells) did not exhibit a significant decrease between these two conditions, confirming their potential role as a negative control. **(*Figure 21*)**

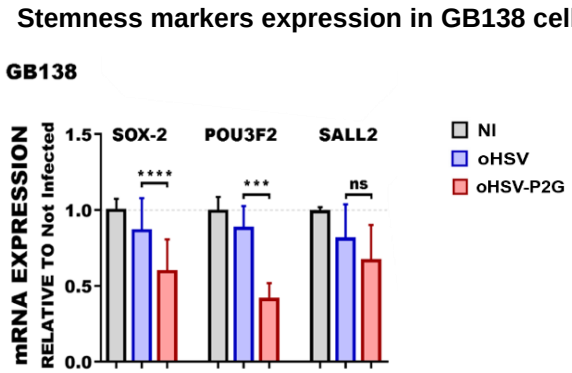

Figure 22 : Stemness markers expression in GB138 cells. mRNA expression of stemness markers in GB138 cells infected with oHSV and oHSV-P2G (Paolo D'Arrigo, post-doc)

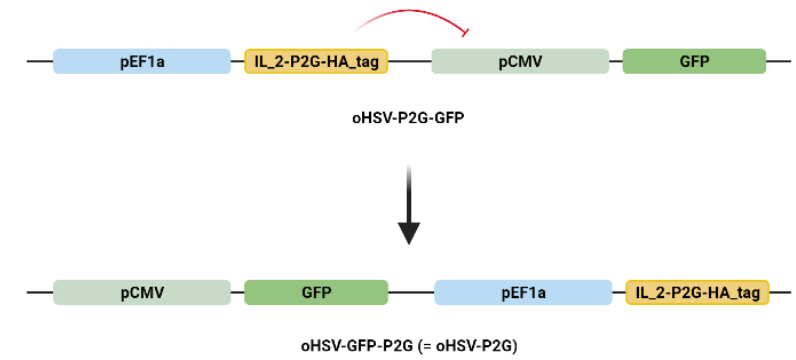

Figure 23 : Change in oHSV-P2G genome structure. Schematic representation of the order of transgenes (pCMV-GFP, pEF1a-P2G) in oHSV-P2G-GFP and oHSV-P2G genome. The insertion of pEF1a-P2G transgene in oHSV genome before pCMV-GFP transgene seemed to disturb production of GFP by infected cells. The insertion of pEF1a-P2G transgene in oHSV genome after pCMV-GFP transgene (oHSV-P2G) restored GFP expression and didn't disturb P2G expression. *Created with BioRender.com*

The clonogenic assay is another way to evaluate the self-renewal abilities of GBM cells but focusing on the cell lines growing in 2D. It consists in plating a specific number of not infected, as well as oHSV and oHSV-P2G infected cells (plating after 18h of infection), and counting the number of colonies formed after 7 days (following PFA 4% fixation and crystal violet staining). This assay successfully demonstrated a significant decrease in % plating efficiency ($= \frac{\text{Number of colonies}}{\text{Number of plated cells}} * 100$) for GB138 primary cells infected with oHSV-P2G compared to oHSV infected cells. **(*Data not shown*)**

Subsequently, stemness markers mRNA expression (SOX-2, POU3F2, SALL2) were analysed by RT-qPCR in GB138 cells after undergoing a spheroid assay. This assay showed a significant decrease in the case of SOX-2 and POU3F2 as well as a decreasing trend for SALL2, though not significant, in line with the data from the spheroid assay. **(*Figure 22*)**

These effects on stem-like features of GBM cells show the decrease in GSCs in GBM cell lines treated with P2G, resulting from an effective inhibition of CXCL12/CXCR4 pathway. Thus, CXCL12/CXCR4-mediated migration abilities of GBM cell lines, which are related to the presence of GSCs, could likely be impacted by oHSV-P2G treatment.

2. Master Thesis Results

2.1. Engineering of oHSV-P2G

The expression of GFP by oHSV allows easy, and almost direct, observation and tracking of viral infection *in vitro*. oHSV-P2G was previously engineered by inserting the pEF1a-P2G transgene before the pCMV-GFP one (this virus will be called here oHSV-P2G-GFP). However, the insertion of this transgene in oHSV genome lead to a decrease in the expression of GFP (and thus a decrease in the observed fluorescence) in oHSV-P2G-GFP and, thus, difficulties in viral infection observation. This issue could be explained by an interference between the newly inserted pEF1a-P2G transgene and the pCMV promoter. Thus, the first step of the master thesis consisted in trying a new construction for oHSV-P2G by inserting the pEF1a-P2G transgene after pCMV-GFP to avoid any interference and to obtain a oHSV-P2G expressing GFP (oHSV-GFP-P2G, called oHSV-P2G for simplification). **(*Figure 23*)**

By-passing cloning of oHSV-P2G

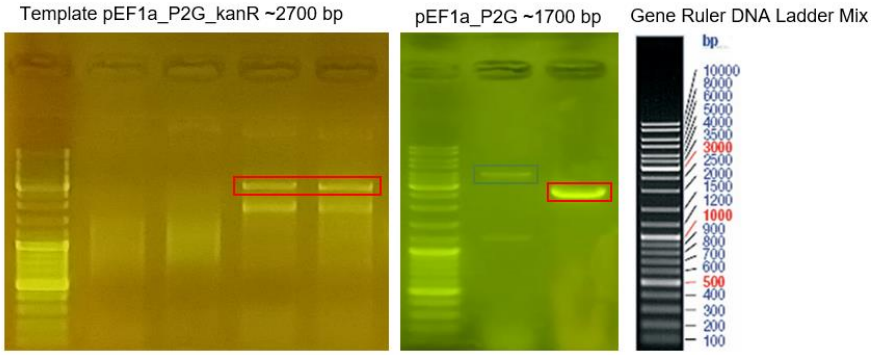

Figure 24 : By-passing cloning of oHSV-P2G. 1) *Template pEF1a_P2G_kanR ~2700 bp,* AGE following PCR amplification of the insertion cassette from the pEF1a-P2G plasmid before first Red recombination (in the red frame, DNA band extracted for transformation). 2) *pEF1a_P2G ~1700 bp,* AGE following PCR amplification of the insertion cassette after second Red recombination (in the red frame, DNA band without kanR sequence ; in the green frame, DNA sequence with kanR sequence). 3) Gene Ruler DNA Ladder Mix representation.

Production of P2G (HA-tag) in cell and media of infected GB138 and GL261 N^+ cells

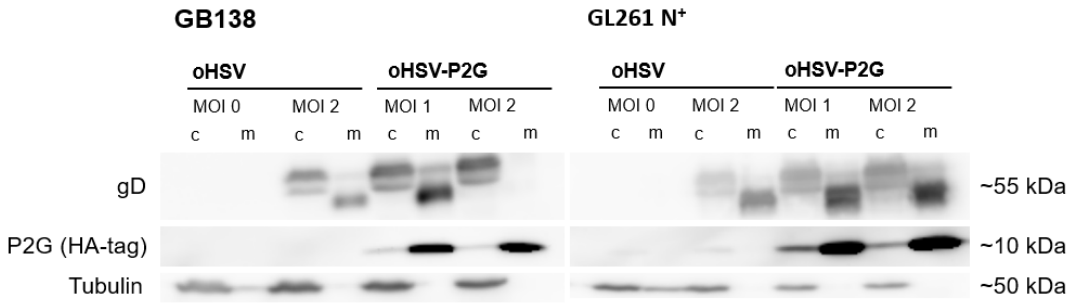

Figure 25 : Production of P2G (HA-tag) in cell and media of GB138 and GL261 N^+ infected cells. Western Blotting analyses of HA-tagged P2G production in GB138 cells after 18h of infection by oHSV-P2G as well as not infected and infected by oHSV as control.

This new construction was made by by-passing cloning. The insertion cassette containing pEF1a-P2G transgene with a kanR selection marker was amplified by PCR from the pEF1a-P2G plasmid. *Escherichia Coli* GS1783 electro-competent bacteria containing the oHSV BAC were transformed with the PCR product and the transgene was integrated in the BAC by a first Red recombination. Successful integration of the template pEF1a-P2G_kanR sequence in the BAC was confirmed by colony PCR followed by AGE and several clones were selected for the second Red recombination. The latter allowed the removal of the kanR selection marker from the BAC sequence. Similarly to the previous step, colony PCR and AGE allowed to select the successfully cloned bacteria containing only pEF1a-P2G in their BAC sequence which were sent to sequencing in order to spot potential single mutations. **(*Figure 24*)**

One selected BAC was further purified by Bacmid maxipreparation and transfected in VERO cells for viral production. Finally, oHSV-P2G was purified and concentrated by ultracentrifugation before being conserved at -80°C, thawed, and titrated (titer=$5.92x10^5$ pfu/µL). In parallel, in order to have sufficient viral stocks as well as to work with viruses titrated in conditions as similar as possible, oHSV was used to infect VERO cells for viral production, purified by ultracentrifugation and titrated at the same time as oHSV-P2G (titer=$5.74x10^6$ pfu/µL, ~10 times more concentrated than oHSV-P2G). In the end, the two viral stocks were conserved at -80°C in aliquots of 10-25 µL. Note that the viral infection of VERO cells showed that the newly produced oHSV-P2G expressed GFP as efficiently as oHSV.

2.2. P2G production verification

Before characterizing the effect of the newly produced GFP-expressing oHSV-P2G, it was important to confirm the expression of P2G. Indeed, if the expression of GFP was inhibited by the insertion of a transgene before its promoter, the same could impair the expression of P2G.

The production of P2G inside GBM human (GB138) and murine (GL261 N^+) cell lines and in their culture media (to confirm successful secretion) was analysed by western blotting after 18h of infection. P2G transgene contains an HA-tag which allow easy recognition using an anti-HA antibody. The assay showed successful production of P2G in oHSV-P2G infected cells and media as well as its absence in oHSV-infected and not infected cells and media as control. **(*Figure 25*)**

Besides, the quantity of P2G is visually higher in the media than in the cellular extracts. However, the intensity levels are not to be compared as the wells with cell extracts contain exactly 80 µg of proteins while the wells with media contain the whole protein extract from the corresponding media.

Tubulin, which is encoded by a cellular housekeeping gene, was used as loading control to ensure equal amounts (in µg) of cellular extracts had been loaded and transferred across all wells of the Western blot. In the second well for both GB138 and GL261 N^+ cells, tubulin can be observed indicating a contamination of the media extract by cellular proteins (this contamination is only observed in the case of not infected cells).

Finally, gD was observed to confirm that the samples had been successfully infected or not according to the protocol. Surprisingly, gD antibody seems to recognize a protein in the media extract which is not the same size as gD from cell extract (potentially a form of gD that could be secreted, cleaved or with different glycosylation pattern). **(*Figure 25*)**

2.3. P2G-containing conditioned media production

As mentioned previously, the assays on oHSV-P2G effect on GBM cell lines migration and invasion were performed using conditioned media derived from not infected (NI conditioned media), oHSV-infected (WT conditioned media), or oHSV-P2G (P2G conditioned media) infected GB138 primary cells after 48h of incubation in DMEM/F-12 without growth factors media. The decision to work with conditioned media was taken in order to avoid the direct effect of infection and cell lysis on cell migration abilities, as well as to focus on the effect of P2G produced in the media during infection. For example, the direct effect of infection can be observed in preliminary results on stem-like features of GBM cell lines. **(*Figure 21, 22*)** NI conditioned media was used as control to measure relative variation between similar conditions. NI+AMD3100 (NI media added with 25 nM of AMD3100) was used as a control for the effect of a known potent FDA-approved CXCR4/CXCL12 pathway inhibitor. WT conditioned media was used as control for the effect of media derived from usual infection on migration and invasion abilities. Indeed, some molecules could be produced by cells upon infection affecting several cell properties. In fact, it was observed in all cases that some growth factors produced during the 48h of culture were sufficient to inhibit migration and invasion. The conditioned media was thus diluted 1:1 by DMEM/F-12 media without growth factors in all further experiments.

To focus on the direct effect of P2G on cell migration and to discriminate this effect from the one mediated by the infection and the cell lysis, conditioned media was used for most experiments. Media derived from not infected (NI conditioned media), oHSV-infected (WT conditioned media), or oHSV-P2G (P2G conditioned media) infected GB138 primary cells were thus harvested after 48h of incubation in DMEM/F-12 without growth factors media, centrifuged, aliquoted and stored at -20°C. The conditioned media was then diluted 1:1 by DMEM/F-12 media without growth factors in all further experiments. NI conditioned media was used as control to measure relative variation between similar conditions. NI+AMD3100 (NI media added with 25 nM of AMD3100) was used as a control for the effect of a known potent FDA-approved CXCR4/CXCL12 pathway inhibitor.

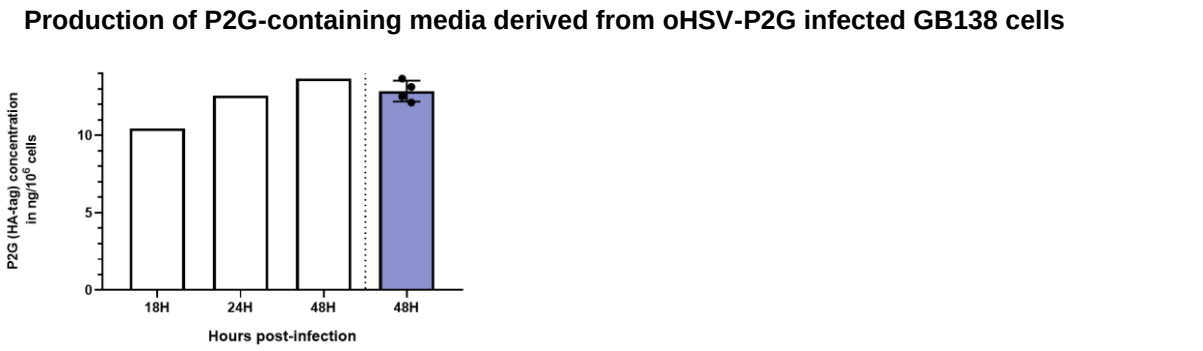

***Figure 26 : Production of P2G-containing media derived from oHSV-P2G infected GB138 cells*.** ELISA assay quantifying the concentration (ng/10^6 cells) of HA-tagged P2G in media derived from oHSV-P2G infected cells, centrifugated and filtered (0.1 µm) to remove all viral particles. First three columns show the increase in concentration over time for one single media production. The forth column show mean concentration of four independent productions.

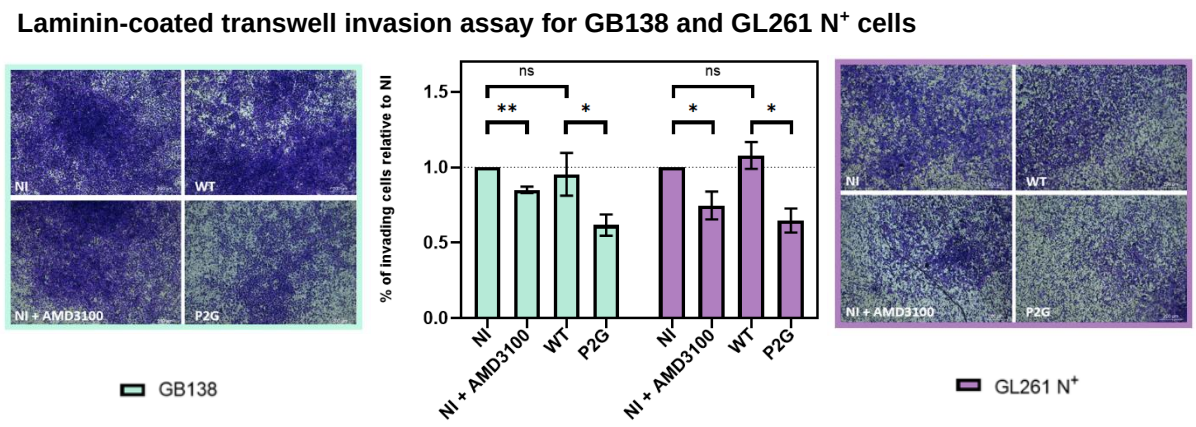

Figure 27 : Laminin-coated transwell invasion assay in GB138 and GL261 N+ cells. Laminin-coated transwell invasion assay with GB138 and GL261 N^+ cells incubated, in the upper chamber, in 50:50 DMEM media without growth factors and conditioned media derived from not infected (NI), oHSV infected (WT), and oHSV-P2G (P2G) infected GB138 cells. Cells are attracted by DMEM HG 10% FBS in the lower chamber. AMD3100 is used as a control inhibitor in NI and WT as a control for the potential effect inherent to infection derived media. Graphs are mean values + SEM and are representative of 3 independent experiments. *, p-value < 0.05; **, p-value < 0.01; ns, not significant.

Before starting experiments using this conditioned media, the concentration of P2G was measured by ELISA in the different P2G-conditioned media productions. Four different production were carried out and the increase in P2G concentration over time was measured for one of them. The latter analysis showed that P2G production in culture media progressively increases over time. **(*Figure 26*)**. In addition, there was no significant variation in the concentration of P2G in the different productions. P2G final concentration was around 10-15 ng/10^6 cells in culture media after 48h of infection in p175 flasks (~1.8x10^7 cells at 100% confluence) **(*Figure 26, blue histogram*)**.

2.4. Characterization of oHSV-P2G effect on GBM cells migration abilities

2.4.1. oHSV-P2G effect on 2D GBM primary cells invasion (GB138 ; GL261 N⁺)

The previously described conditioned media (NI, NI+AMD3100, WT, P2G) were used in laminin-coated transwell invasion assays with GB138 and GL261 N^+ cells. This assay aims to mimic ECM invasion of cancer cells which is an essential step in cancer metastasis. For this assay, it is necessary to work with single dissociated cells. GB138 and GL261 N^+ cells growing fast as monolayers and easily dissociated are thus perfectly suited for this assay. Based on previous trials aiming at the optimisation of the number of cells to seed, 20k GB138 and 25k GL261 N^+ cells were plated in the transwell upper chamber and incubated in 1:1 conditioned media and DMEM/F-12 media without growth factor. The cells in the upper chamber are potentially attracted towards the lower chamber containing DMEM HG 10% FBS media. After 48h, cells that have migrated towards the lower chamber and visible on the bottom side of the transwell are with PFA 4% and stained with crystal violet. This staining allows picture to be taken with optical microscope and counting of invading cancer cells. Data are displayed relatively to NI conditioned and the % of invading cells is measured as $\frac{Number\ of\ invading\ cells}{Number\ of\ plated\ cells} * 100$.

In both cases (GB138 and GL261 N^+), a significant decrease of cell invasion was observed in NI+AMD3100 compared to NI conditioned media and in P2G compared to WT conditioned media. Note that the decrease observed for NI+AMD3100 is lower than for P2G, but this disparity is significant only in the case of GB138 cells **(not shown on Figure 27)**. Furthermore, it is also important to take into account that no significant differences can be seen between NI and WT media. **(*Figure 27*)**

Spheroid migration assay for T013 and T08 cells

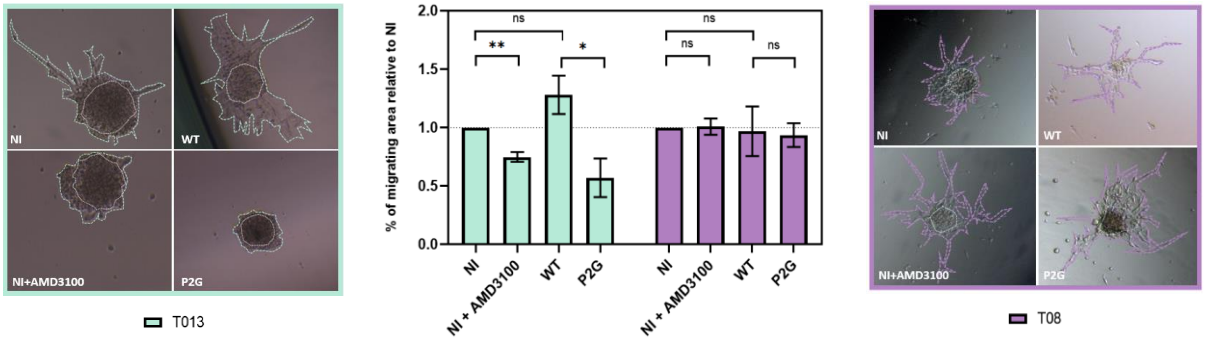

Figure 28 : Spheroid migration assay for T013 and T08 cells. Spheroid migration assay with T013 and T08 neurospheres incubated in 50:50 DMEM media without growth factors and conditioned media derived from not infected (NI), oHSV infected (WT), and oHSV-P2G (P2G) infected GB138 cells. AMD3100 is used as a control inhibitor in NI and WT as a control for the potential effect inherent to infection derived media. T08 cells are used as control for the effect of CXCL12 inhibitors on low CXCR4 expressing cells. Images of the experiment on the side of the graph are representative of triplicates. Graphs are mean values + SEM and are representative of 3 independent experiments. *, p-value < 0.05; **, p-value < 0.01; ns, not significant.

2.4.2. oHSV-P2G effect on 3D GBM primary cells migration (T013 ; T08)

2.4.2.1. Spheroid migration assay

Conditioned media were used also for spheroid migration assays with T013 and T08 cells. This assay aims to mimic in the best possible way the migration of cells away from the tumour mass, which is happening for example when GSCs migrate towards the SVZ. For this reason, the use of 3D neurospheres has been favoured. These spheroids are cultured in 96-well plate previously coated with poly-D-lysine to allow their adherence to the well surface and their spontaneous migration further occurs spontaneously on the coated plate. In the same way as for the invasion assay, the spheroids adhering to the plate were incubated for 48h in conditioned media and DMEM/F-12 media without growth factor (1:1). After 48h, the area of migration is measured and compared to the initial spheroid size. Data are displayed relatively to NI conditioned and the % of migrating area cells is measured as $\frac{Area\ 48h - Area\ 1h}{Area\ 48h} * 100$.

For T013 cells, a significant decrease of cell migration was observed in NI+AMD3100 compared to NI conditioned media and in P2G compared to WT conditioned media (even though the decrease is lower in for NI+AMD3100 than for P2G). Furthermore, it is also important to note that no significant difference can be seen between NI and WT media although an increasing trend can be observed in favour of WT conditioned media. On the other hand, T08 cells in the exact same assay exhibit no significant differences of migration in the different conditions. This was expected as T08 cells in culture show a very low proportion of CXCR4 expressing cells. **(*Figure 28*)**

2.4.2.2. Vimentin immunofluorescence

At the end of the spheroid migration assays, some spheroids were fixed with PFA 4% before being stained. This assay aims to evaluate whether the expression of vimentin, which is a migration marker, is modulated upon treatments. Nucleus were stained with Hoechst in order to have an easy visual appreciation of the distribution of the cells on the pictures and, mainly, to visualise cells with low intensity of vimentin fluorescence. Pictures are taken by confocal microscopy and the intensity of fluorescence is measured using ImageJ.

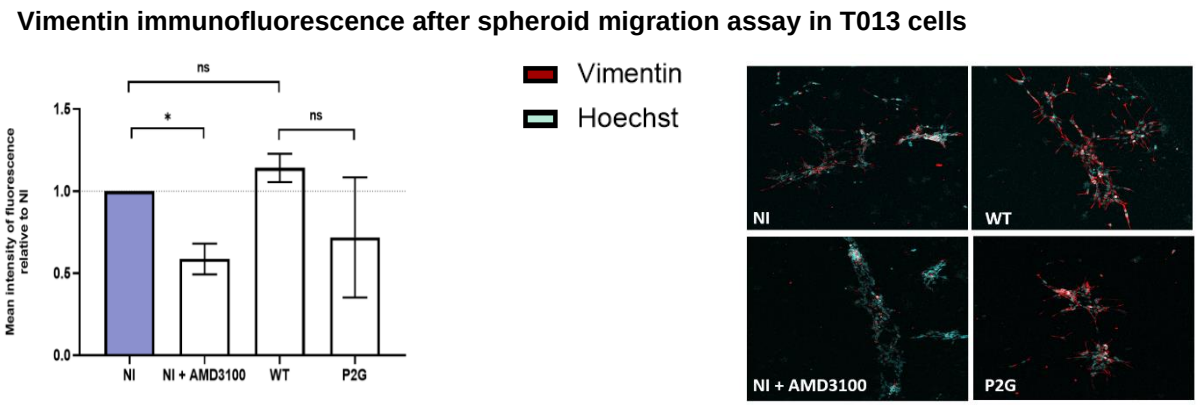

***Figure 29 : Vimentin immunofluorescence after spheroid migration assay in T013 cells*.** Vimentin immunofluorescence after spheroid migration assay with T013 neurospheres incubated in 50:50 DMEM media without growth factors and conditioned media derived from not infected (NI), oHSV infected (WT), and oHSV-P2G (P2G) infected GB138 cells. AMD3100 is used as a control inhibitor in NI and WT as a control for the potential effect inherent to infection derived media. Image of the experiment on the side of the graph is representative of the triplicate (Vimentin in red and Hoechst in cyan). Graphs are mean values + SEM and are representative of 3 independent experiments. *, p-value < 0.05; ns, not significant.

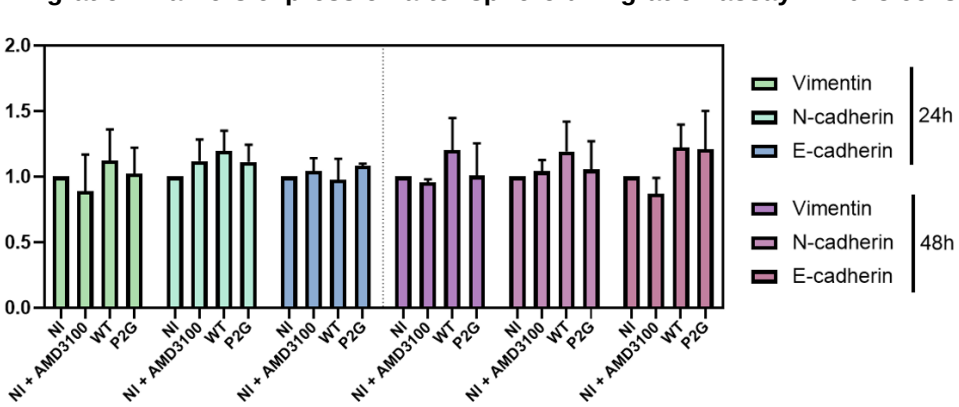

Figure 30 : Migration markers expression after spheroid migration assay in T013 cells. mRNA expression measured by RT-qPCR of migration markers (vimentin, N-cadherin, E-cadherin) after 24h, 48h of spheroid migration assay with T013 neurospheres incubated in 50:50 DMEM media without growth factors and conditioned media derived from not infected (NI), oHSV infected (WT), and oHSV-P2G (P2G) infected GB138 cells. AMD3100 is used as a control inhibitor in NI and WT as a control for the potential effect inherent to infection derived media. Graphs are mean values + SEM and are representative of 3 independent experiments.

These experiments were performed at the end of spheroid migration assay with T013 cells. A significant decrease in vimentin fluorescence intensity was observed in NI+AMD3100 compared to NI conditioned media. Furthermore, there were no significant differences between NI and WT media. Surprisingly, no significant decrease could be observe with P2G conditioned media compared to WT. Moreover, despite a decreasing trend, the difference between the WT and P2G treated spheroid was not significant, due to an important variation between replicates for P2G conditioned media. Moreover, it is difficult to discern any intensity decrease in visual representation of the experiment. **(*Figure 29*)**

2.4.2.3. Migration markers mRNA expression

At the end of the spheroid migration assays, some spheroids were collected for total RNA extraction followed by RT-qPCR to analyse mRNA expression of migration markers (vimentin, N-cadherin, E-cadherin). This assay aims to characterize the evolution of migration markers expression at the mRNA level following the variation in migration phenotype. We could expect to see: 1) a positive correlation between vimentin or N-cadherin mRNA expression and migration level (thus, a decrease of those markers in line with the decrease in migration), and 2) a negative correlation between E-cadherin mRNA expression and migration level (as N-cadherin and E-cadherin are supposed to vary in opposite ways as described in the cadherin switch during EMT). The spheroids are left to migrate for 24h or 48h in order to monitor the timing of mRNA expression modulation, as it may precede the apparition of the phenotype (which was observed after 48h).

Although these experiments were performed with T013 cells in the same conditions as the spheroid migration assay, no significant variation could be observed in any of the conditions neither for 24h nor 48h. Furthermore, important variation occurred between the different replicates completely preventing observation of any significant results. **(*Figure 30*)**

V. Discussion and perspectives

1. Focus on GBM cells migration abilities and oHSV-P2G engineering

Glioblastoma multiforme is an aggressive high-grade astrocytoma (WHO, grade IV). Current standard treatments consist in maximal surgical resection followed by chemo-/radio- therapy. Unfortunately, this treatment protocol is impaired by systematic tumour reformation. These relapses were found to be related to GSCs/GICs able to escape resection by migrating from the tumour mass to the SVZ through the CC, following a CXCL12 gradient. Migration of GSCs is thus a crucial aspect that needs to be addressed when searching potential new treatments against GBM able to prevent those recurrences. Note that this focus on migration follow preliminary results showing a decrease in GSCs presence, and inhibition of GBM cells stem-like features, upon inhibition of CXCL12/CXCR4 pathway using oHSV-P2G. During this master thesis, migration abilities of different GBM cell lines were analysed *in vitro* in different experimental conditions in order to evaluate the effect of P2G.

This master thesis, which focuses on GBM cells migration, is part of a larger project. The objective of the latter is to develop a new therapy (virotherapy) against GBM, mainly in the aim of preventing recurrences following standard treatment. Virotherapy is used to target cancer cells and cause their lysis, but is also useful to modulate the immune response.

In the future, the effects of oHSV-P2G will have to be evaluated *in vivo*. Two mice models are currently used in the literature and at the laboratory. One is a xenograft athymic nude mouse model lacking adaptive immune system. The other is a syngeneic immunocompetent C57BL/6 mouse model. On the one hand, the nude mice model can be injected with human GBM cell lines. This allows to work with various human primary GBM cells which is important to approach the diversity observed among GBM tumours. Indeed, GBM are highly heterogeneous both between patients and within a single tumour. Nevertheless, the lack of adaptive immune response is an important drawback, especially in the case of virotherapy which is known to trigger the immune response that participates to the tumour eradication. On the other hand, the immunocompetent model solves this issue and permits analysis of the immune response upon treatment. However, this model implies the use of murine GBM cells and do not allow the injection of human cells.

For this reason, various primary human GBM cells (GB138, T013, T08) and a murine GBM cell line (GL261 N^+) were used during this master thesis. In this way, *in vitro* results will show some diversity of primary human GBM cells and be more representative of GBM heterogeneity. Furthermore, *in vitro* assays will provide essential preliminary results on murine GBM cell lines before *in vivo* experiments in syngeneic mouse model. GB138 and GL261, previously transduced with the human nectin to make them more susceptible to HSV-1 infection (GL261 N^+), have the advantage that they can be cultured in 2D in DMEM HG FBS 10% or in 3D in neurosphere media. T08 and T013 cells can be cultured only in 3D but easily form neurosphere which are closely similar to *in vivo* tumours. T08 cells are GBM tumour mass primary cells showing low expression of CXCR4 at the cell membrane. Thus, they are used as a negative control for P2G effect on cell migration and migration markers.

Before assessing the effect of P2G on migration, oHSV-P2G had to be engineered. oHSV-P2G was constructed successfully by "by-passing" cloning from a BAC containing the oHSV genome (previously deleted for ICP34.5, ICP6, and ICP47) and a plasmid with pEF1a-P2G sequence. The insertion cassette containing the latter was introduced after pCMV-GFP cassette already present in the viral genome used as backbone. Viral infection of VERO cells showed that the newly produced oHSV-P2G (= oHSV-GFP-P2G) expressed GFP as efficiently as oHSV. Moreover, both human GBM primary cells (GB138) as well as murine GBM cell lines (GL261 N^+) successfully produced P2G during infection as verified by Western Blotting and quantified by ELISA.

Surprisingly, when revealed with an anti-gD antibody to verify the level of infection, the western blot analysis, revealed the presence, in the supernatant of a protein with a smaller size (in Da) than gD in infected cellular extracts. This observation was even more surprising as this protein is not present in all infected cell media **(*Figure 25 GB138 oHSV-P2G MOI 2 m*)**. This recognized protein could be attributed to a secreted, cleaved or differently glycosylated, form of gD. However, such a protein was not found to be reported in the literature.

All in all, the presence of this alternative form of gD does not affect the expected results concerning the successful production of P2G by oHSV-P2G. In the same way, the contamination of media extract by cellular proteins in the case of not infected cells do not affect the interpretation of the results.

Several conditioned media (NI, NI+AMD3100, WT, P2G) were produced and filtered (0.1 µm filter) in order to remove all viral particles and avoid any infection, allowing thereby the evaluation of the impact of P2G itself. Analyses of those productions allowed to confirm that the concentration of P2G was quite similar in all conditioned media (~10-15 ng/10^6 cells). Moreover, the concentration of P2G increased over time in both the supernatant and the cell extracts.

NI conditioned media was used as a standard migration condition (measures are all given relatively to NI). NI+AMD3100 media was used as a control for the effect of a known FDA-approved CXCL12/CXCR4 pathway inhibitor. WT conditioned media was used as control for the effect of media derived from non-armed oHSV infection. Indeed, some molecules could be produced by cells upon infection and potentially have an impact on cell migration. Indeed, we observed that some growth factors produced during the 48h of culture were sufficient to inhibit migration and invasion abilities. Experiments were thus performed using conditioned media diluted in DMEM/F-12 without growth factors media (1:1). Besides, WT media was also be compared to NI to see if media derived from oHSV infection inherently have an effect on GBM cell migration.

2. Results limitations

The impact of P2G on GBM cells migration has been evaluated using three approaches: transwell experiment (laminin-coated invasion assay), spheroid migration assay and evaluation by RT-qPCR of some migration markers. Before drawing any general conclusions from the obtained results, it is important to understand the limitations of each experiments. Some of those limitations are inherent to the experiment, some are due to technical issues or restricted time, and some were unexpected.

For instance, all cell lines couldn't be used in each experiment for various reasons. Precisely, transwell assays were performed with 2D GBM cells cultures while spheroid migration assays required 3D GBM cells culture. T08 and T013 do not grow as monolayers and grow as 3D neurospheres quite slowly. They were thus not used in all assays but were used when absolutely necessary (spheroid migration, vimentin immunofluorescence, migration markers expression assays). In the future, these assays will of course have to be repeated in all cell lines.

2.1. Laminin-coated transwell invasion assay

Conditioned media were used to assess the effect of P2G on invasion abilities of GBM cells, which were analysed by laminin-coated invasion assay. Laminin is used here to mimic the ECM and the process of invasion occurring *in vivo*. This invasion assay can only be performed with dissociated single cells. Thus, GBM cells growing as 2D monolayers (GB138, GL261 N^+) were first used for their rapid growth and the ease with which they can be dissociated, counted and plated.

A technical issues was to find the right number of cells to be plated and the invasion timing. The timing of 48h that was used for final experiments was determined after settings experiments with three time points (18h, 24h, 48h). Indeed, it seemed that 18h and 24h did not offer the time needed for cell invasion. For the number of cells, settings experiments were first performed plating 50k or 25k cells. However, plating of 50k cells led to saturated transwell membranes and uninterpretable results. Another issue was that the proportion of invading GB138 cells was higher than the one of GL261 N^+ cells. Indeed, at 25k plated cells some saturation of the membrane was still observed for GB138 cells. However, the results obtained with the same number of cells for GL261 N^+ cells were satisfying. It was thus decided to plate a different number of cells for each cell lines and reduce the number of plated GB138 cells to 20k. As described in the results, 20k GB138 cells and 25k GL261 N+ cells were finally plated for each experiment. In fact, the number of plated cells could certainly have been reduced even more for both cell lines. This might have facilitated the counting of the invading cells and the interpretation of the results. However, these results significantly indicate that P2G impairs GBM cell invasion abilities.

Some alternative settings were also considered in the aim of enhancing the scope of the assay. The proportion of $CXCR4^+$ GB138 and GL261 N^+ cells was shown to increase when cells are cultured in 3D compared to the same cells cultured in 2D. This could increase the observable effect of CXCL12/CXCR4 pathway inhibitors on those cell populations. Thus, it was considered to grow GB138 and GL261 N^+ cells as 3D spheroids in neurosphere media, before dissociating and using them for the transwell assay, with the same previously determined settings. The higher proportion of $CXCR4^+$ (= higher proportion of invading cells) resulted in completely saturated membranes with 25k plated cells. Therefore, it would be necessary to re-optimise the settings of the experiment before using this alternative method.

Another possibility that was taken into consideration was to add 500 nM of CXCL12 to the lower chamber to create a gradient forcing the cells to migrate. Such setting would allow to evaluate the competition between CXCL12 and P2G for binding CXCR4, hopefully resulting in a decrease of CXCL12 global chemotactic effect The concentration of CXCL12 was selected according to the literature.1 Indeed, with DMEM HG 10% FBS in the lower chamber, invasion from the upper to the lower chamber is not only driven by mechanisms related to the CXCL12/CXCR4 pathway. This reduces the proportional effect on migration of CXCR4/CXCL12 pathway inhibitors. Nevertheless, due to the lack of time, this experiment has been performed only once and almost no invading cells were observed in those conditions indicating that the settings had to be adjusted (e.g. increasing the timing, the number of plated cells, the concentration of CXCL12 in the lower chamber).

2.2. Spheroid migration assay

Conditioned media were also used to assess by spheroid migration assay the effect of P2G on GBM primary cells migration abilities of GBM primary cells. Human GBM primary cells growing as 3D neurospheres (T08, T013) were used in this assay. This assay mimics migration of cancer cells at the edge of the tumour mass, as it occurs *in vivo* during cancer spreading and metastasis. GB138 and GL261 N^+ could also be used for this assay as they can be grown as 3D neurosphere. This will have to be performed in the future.

Some technical issues were also faced for this assay. First, some spheroids never get fixed on the poly-D-lysin coated plate and migration area could not be measured for those spheroids. Furthermore, neurospheres do not grow evenly. Little spheroids completely spread on the plate after 48h (no more neuropshere, but only 2D single cells observed in the plate) which makes it impossible to measure the area of migration. On the other hand, too large spheroids seem to adhere less efficiently to the poly-D-lysine coated plate and to migrate proportionally less than spheroids with intermediate size. This problem was solved by using centrifugation (or letting spheroids pellet by gravity) cycles to select for spheroids with intermediate size. This issue was also partly solved by growing neurospheres in culture for a shorter time, preventing the formation of too large spheroids. These steps were necessary to obtain interpretable results and reduce the standard deviation within one condition. These results significantly indicated that P2G impairs T013 cells migration. Nevertheless, T08 cells (showing low proportion of $CXCR4^+$ cells in their population) migration was not inhibited by P2G demonstrating the specificity of the treatment for the CXCR4/CXCL12 pathway.

Some assays using GB138 and GL261 N^+ were also performed. However, these experiments still need to be repeated before being submitted to statistical analysis. In fact, neurospheres formed by those cell lines are quite unstable and some cells dissociate on their own from the spheroid when they are manipulated. This result in the presence of a lot of single cells in the wells during migration. It becomes thus complicated to differentiate cells migrating from a neurospheres and the, also migrating, adhering single cells. Therefore, measure of the area of migration and interpretation of the results has been troublesome.

Finally, similar experiments could be performed using live-cell analysis systems (e.g. IncuCyte®). Indeed, some protocols involving the IncuCyte® allow the observation of one single spheroid per well (96-well plate). The increase in the migration area can then automatically be measured over time and visualise as time lapse video. This could allow more precise measurements than the one obtained using ImageJ. Besides, on its own the use of time lapse video could help in solving the problem of the differentiation between cells migrating from a neurospheres and the adhering single cells.

2.3. Migration markers observation

The significant results, obtained with T013 cells in the spheroid migration assay, encouraged us to analyse the expression of migration marker at the end of this assay. After 48h of migration, spheroids were collected for vimentin immunofluorescence assay and mRNA expression of migration markers (vimentin, N-cadherin, E-cadherin) analysis by RT-qPCR. Nevertheless, the effect of P2G on migration could not be confirmed at the molecular level by the observation of those migration markers (vimentin, cadherins) in neither of these experiments.

2.3.1. Vimentin immunofluorescence assay

For the vimentin immunofluorescence assay, the decrease in mean intensity of fluorescence was significant for NI+AMD3100 media compared to NI, but not for P2G compared to WT. This absence of significance seems to be due to the important standard variation observed between the three replicates in P2G conditioned media.

Nevertheless, it also might be that this assay is not suited to assess the variation of migration markers at the protein level. The main advantage of this experiments was to obtain a picture and be able to observe cellular vimentin organisation. Indeed, it is suggested in the literature that vimentin does not directly increase cell migration but enhance its directionality by polarizing the cells.[59] Thus, a decrease in the phenotype of migration could be due to some disorganisation of vimentin preventing this polarisation of the cell. Such disarrangement was not observed in any conditions. However, a clear decrease in the mean intensity of vimentin fluorescence could be visualised and measured for NI+AMD3100 conditioned media.

It is surprising not to observe any differences in vimentin (migration marker) expression at the protein level. Indeed, it was expected that vimentin expression would be correlated to the percentage area of migration in the spheroid migration assay. Thus, the up-regulation of vimentin (and cadherins) at the protein level should be observed with alternative methods. For instance, WB or FACS analysis.

2.3.2. Migration markers mRNA expression assay

For the RT-qPCR, even though several time points were used to try to understand the pattern of migration markers mRNA expression over time, no significant results were obtained in any conditions. Besides the 24h and 48h time points, 18h **(*Data not shown*)** was also tried but abandoned as results were similar. A first RT-qPCR was realised using primers hybridizing in a single exon. Therefore, the absence of observable variation of mRNA expression among the different conditions was suspected to result from amplification of DNA instead or in addition to mRNA. Indeed, contamination of the RNA extract with DNA might explain the obtained results. Thus, it was decided to order new primers hybridizing this time onto different exons. This would ensure that contaminant DNA could not be amplified during qPCR. Nevertheless, the new primers did not change previous results.

Once again, it is surprising not to observe any differences in mRNA expression level of migration marker, as a disparity in migration level was observed in the spheroid migration assay. The absence of negative correlation between N-cadherin and E-cadherin, generally described in the literature (see introduction) was also very surprising.

The analysis of the migration markers was pursue by Paolo D'Arrigo following these disappointing results. T013 were incubated for four days in conditioned media before analysing mRNA expression of migration markers. Thus, the cells were not in migration conditions as it was done before by collecting cells at the end of the 48h-long spheroid migration assay. Moreover, the cells were not in conditioned media diluted with DMEM/F-12 without growth factors media (1:1). In these new conditions, an important decrease in vimentin and a high increase in E-cadherin expression were detected upon treatment with P2G conditioned media compared to WT conditioned media **(*Data not shown*)**. However, no decrease in N-cadherin was observed at the transcriptional level. It is possible that some regulation mechanisms could cause variation on a post-transcriptional or post-translational level of N-cadherin. It was indeed described in the literature that N-cadherin is regulated by a cleavage mechanism activating the protein (formation of an active cytoplasmic C-terminal region of ~40kDa) and having an effect on cell adhesion.[62] Such impact on N-cadherin cleavage was investigated by WB after four days of T013 cells incubation in conditioned media. Preliminary data revealed a decrease in the cleaved form of N-cadherin in P2G conditioned media. These assays are to be repeated to confirm this observation and before being submitted to statistical analysis. They still constitutes encouraging steps in showing P2G effect on migration at the molecular level. It would also be interesting to perform a spheroid migration assay with these cells, previously cultured in conditioned media for 4 days and in which vimentin and E-cadherin seem to be modulated. In this way, it might be possible to observe a correlation between the level of migration and the variation in migration markers at the mRNA and post-translational level.

In the future, the above described RT-qPCR and WB will have to be repeated to obtain results that could be submitted to statistical analysis. Consequently, the effect of oHSV-P2G on invasion as well as migration would be demonstrated at the phenotype and the molecular level for different cell lines. Of course, assays will have to be repeated with all cell lines. This will allow us to have more drastic conclusions over the obtained results. Moreover, these results could be completed by observing the effect on migration and invasion of CXCL12 stimulation in non-infected conditions. This would be used as a control before using CXCL12 to rescue migration phenotype in P2G conditioned media. This would definitely prove the implication of CXCR4/CXCL12 pathway in the observed inhibition of migration.

3. Conclusions

General conclusions on the effect of P2G, CXCL12/CXCR4 pathway inhibitor, on GBM cell migration and invasion abilities can thus be drawn from this master thesis. It is important to note that invasion and spheroid migration assays were not performed on the same cell lines. Thus, the effect of P2G on migration and invasion was not completely characterised in any of the used cell lines.

First, the effect of P2G can be compared to the effect of WT conditioned media. P2G significantly inhibited invasion abilities of 2D human primary GBM cells (GB138) and 2D murine GBM cells (GL261 N^+), as well as migration abilities of 3D human GBM primary cells (T013). 3D human GBM primary cells which exhibit low proportion of $CXCR4^+$ cells (T08), were used as negative control showing the specificity of the treatment towards the CXCL12/CXCR4 pathway. Nevertheless, the effect of P2G on migration could not be confirmed at the molecular level by the observation of migration markers (vimentin, cadherins).

Besides, the effect of P2G relatively to WT conditioned media can be compared with the effect of NI+AMD3100 relatively to NI conditioned media. In invasion and spheroid migration assays, the inhibition caused by NI+AMD3100 was less drastic than the one obtained with P2G media. However, this disparity was only significant in the case of the invasion assay performed with GB138 cells. Furthermore, these results do not necessarily demonstrate that P2G is more effective in inhibiting invasion than AMD3100. Indeed, the concentration of AMD3100 could certainly be adjusted in order to obtain a more important inhibition of GBM cells migration and invasion abilities. This was not essential for the purpose of this master thesis. Indeed, what is important to note is that there is a significant decrease observed in invasion and migration assays for NI+AMD3100 compared to NI. This decrease due to a FDA-approved inhibitor of CXCR4/CXCL12 pathway constitutes a validation for both methods.

Afterwards, the effect of WT conditioned media can be compared with the effect of NI conditioned media. Surprisingly, an increase in GBM cell migration abilities was observed in invasion and spheroid migration assays, as well as in vimentin immunofluorescence and migration marker expression assays. Even though it was not significant, the increasing trend observed for migration in WT compared to NI conditioned media raised the question of a potential molecule produced during infection that would increase migration of GBM primary cells. This molecule could either be a cellular signal produced by host cells upon infection or a viral protein. Such a molecule would not be retained by the 0.1 µm filter during conditioned media production. A viral protein which was not mentioned in the description of HSV-1 could be involved in this process. gG is a viral envelope glycoprotein which appears to be non-essential for the virus infectious cycle, has been detected as a secreted glycoprotein (SgG). Both gG and SgG were shown to bind the glycosaminoglycan-binding domain of chemokines such as CXCL12.[63,64] Interestingly, instead of inhibiting chemokine function like usual viral chemokine binding proteins, gG is increasing chemotactic effects of those chemokines.[63,64] Moreover, HSV particles-mediated increase in cell migration was shown to occur independently of binding between gG and CXCL12 (other unknown viral proteins could therefore induce cell migration).[63] The mechanism leading to a higher sensitivity to chemokine stimulation in the presence of gG was explained by its impact on receptor trafficking and oligomerisation. Indeed, gG is able to attach to cell surface glycosaminoglycans and to induce lipid raft clustering. CXCR4 will be increasingly incorporated into these microdomains. This will induce a gG-mediated change in CXCR4 homodimers conformation, consequently altering their intracellular partners. Finally, this will result in a decreased internalisation of CXCR4, accumulation of low-order CXCR4 nanoclusters enhancing CXCR4-CXCL12 signalling functionality.[65]

In the end, gG-mediated decreasing of CXCR4 internalisation can result in an increased effect of CXCR4/CXCL12 signalling, and, finally, increased migration abilities of GBM primary cells in WT conditioned media compared to NI.

As a conclusion, P2G effectively inhibited CXCR4/CXCL12 thereby decreasing GSCs migration and invasion abilities in different primary GBM cells as well as in murine GBM cell line. However, the performed experiments need to be repeated with all available cell lines to confirm these general conclusions.

4. Perspectives

Although these experiments have to be repeated with different cell lines, the results obtained so far are encouraging and indicate that P2G can impair GBM cells migration. The effect of oHSV-P2G on migration (as well as other features, such as stemness, angiogenesis, etc) will then be further investigated *in vivo*. For instance, *in vivo* analysis could be performed on murine brain slices obtained from mice engrafted with GBM cells and treated with intratumoral injection of the virus (P2G-armed or not). This could allow the observation and the quantification of GBM cells escaping the tumour mass and eventually migrating to the SVZ. In a xenograft nude mouse model, injected human GBM cells can easily be observed by immunohistochemistry by targeting human vimentin or human nuclei proteins. In a syngeneic immunocompetent C57BL/6 mouse model, it might be necessary to use RFP^+ murine GBM cells to differentiate them from murine healthy cells (even though GL261 N^+ might be observed by targeting human nectin by immunohistochemistry). The expected results of such an experiment would be to observe a decrease in the number of cells migrating escaping the tumour mass upon treatment with oHSV-P2G. Alternatively, this *in vivo* observation could also be performed using LightSheet microscopy. This technique absolutely requires RFP^+/GFP^+ GBM cells. Following clarification of the murine brains, this technique would allow the observation in 3D of the brain.

References

1. Goffart, N. *et al.* Adult mouse subventricular zones stimulate glioblastoma stem cells specific invasion through CXCL12/CXCR4 signaling. *Neuro. Oncol.* **17**, 81–94 (2015).

2. Goffart, N. *et al.* CXCL12 mediates glioblastoma resistance to radiotherapy in the subventricular zone. *Neuro. Oncol.* **19**, 66–77 (2017).

3. Põlajeva, J. *et al.* Mast cell accumulation in glioblastoma with a potential role for stem cell factor and chemokine CXCL12. *PLoS One* **6**, (2011).

4. Sattiraju, A., Sai, K. K. S. & Mintz, A. Glioblastoma stem cells and their microenvironment. in *Advances in Experimental Medicine and Biology* vol. 1041 119–140 (Springer New York LLC, 2017).

5. Krishna, K. V., Dubey, S. K., Singhvi, G., Gupta, G. & Kesharwani, P. MAPK pathway: Potential role in glioblastoma multiforme. *Interdisciplinary Neurosurgery: Advanced Techniques and Case Management* vol. 23 (2021).

6. Rong, Y., Durden, D. L., Van Meir, E. G. & Brat, D. J. 'Pseudopalisading' Necrosis in Glioblastoma: A Familiar Morphologic Feature That Links Vascular Pathology, Hypoxia, and Angiogenesis. *J. Neuropathol. Exp. Neurol.* **65**, 529–539 (2006).

7. Reardon, D. A. & Wen, P. Y. Therapeutic Advances in the Treatment of Glioblastoma: Rationale and Potential Role of Targeted Agents. *Oncologist* **11**, 152–164 (2006).

8. Stupp, R. *et al.* Effects of radiotherapy with concomitant and adjuvant temozolomide versus radiotherapy alone on survival in glioblastoma in a randomised phase III study: 5-year analysis of the EORTC-NCIC trial. *Lancet Oncol.* **10**, 459–466 (2009).

9. Rominiyi, O. *et al.* Tumour treating fields therapy for glioblastoma: current advances and future directions. *British Journal of Cancer* vol. 124 697–709 (2020).

10. Jackson, M., Hassiotou, F. & Nowak, A. Glioblastoma stem-like cells: At the root of tumor recurrence and a therapeutic target. *Carcinogenesis* vol. 36 177–185 (2014).

11. Ping, Y. F. *et al.* The chemokine CXCL12 and its receptor CXCR4 promote glioma stem cell-mediated VEGF production and tumour angiogenesis via PI3K/AKT signalling. *J. Pathol.* **224**, 344–354 (2011).

12. Wang, S. *et al.* CXCL12-induced upregulation of FOXM1 expression promotes human glioblastoma cell invasion. *Biochem. Biophys. Res. Commun.* **447**, 1–6 (2014).

13. Rao, S. *et al.* CXCL12 mediates trophic interactions between endothelial and tumor cells in glioblastoma. *PLoS One* **7**, (2012).

14. Uemae, Y. *et al.* CXCL12 secreted from glioma stem cells regulates their proliferation. *J. Neurooncol.* **117**, 43–51 (2014).

15. Liu, Y., Ren, C. C., Yang, L., Xu, Y. M. & Chen, Y. N. Role of CXCL12–CXCR4 axis in ovarian cancer metastasis and CXCL12–CXCR4 blockade with AMD3100 suppresses tumor cell migration and invasion in vitro. *J. Cell. Physiol.* **234**, 3897–3909 (2019).

16. De Clercq, E. Recent advances on the use of the CXCR4 antagonist plerixafor (AMD3100, Mozobil™) and potential of other CXCR4 antagonists as stem cell mobilizers. *Pharmacology and Therapeutics* vol. 128 509–518 (2010).

17. Hira, V. V. V., Van Noorden, C. J. F. & Molenaar, R. J. CXCR4 antagonists as stem cell mobilizers and therapy sensitizers for acute myeloid leukemia and glioblastoma? *Biology (Basel).* **9**, (2020).

18. Martel, S. Learning from our failures in blood-brain permeability: What can be done for new drug discovery? *Expert Opin. Drug Discov.* **10**, 207–211 (2015).

19. Mortezaee, K. CXCL12/CXCR4 axis in the microenvironment of solid tumors: A critical mediator of metastasis. *Life Sciences* vol. 249 (2020).

20. Merino, J. J., Bellver-Landete, V., Oset-Gasque, M. J. & Cubelos, B. CXCR4/CXCR7 molecular involvement in neuronal and neural progenitor migration: Focus in CNS repair. *J. Cell. Physiol.* **230**, 27–42 (2015).

21. Lapidot, T., Dar, A. & Kollet, O. How do stem cells find their way home? *Blood* **106**, 1901–1910 (2005).

22. Koch, M., Lawler, S. & Chiocca, E. HSV-1 Oncolytic Viruses from Bench to Bedside: An Overview of Current Clinical Trials. *Cancers (Basel).* **12**, 3514 (2020).

23. Nakashima, H. & Antonio Chiocca, E. Modification of HSV-1 to an oncolytic virus. *Methods Mol. Biol.* **1144**, 117–127 (2014).

24. Andtbacka, R. H. I. *et al.* Talimogene laherparepvec improves durable response rate in patients with advanced melanoma. *J. Clin. Oncol.* **33**, 2780–2788 (2015).

25. Grigg, C. *et al.* Talimogene laherparepvec (T-Vec) for the treatment of melanoma and other cancers. *Seminars in Oncology* vol. 43 638–646 (2016).

26. Peters, C. & Rabkin, S. D. Designing herpes viruses as oncolytics. *Molecular Therapy - Oncolytics* vol. 2 15010 (2015).

27. Wilcox, D. R. & Longnecker, R. The Herpes Simplex Virus Neurovirulence Factor γ34.5: Revealing Virus–Host Interactions. *PLoS Pathogens* vol. 12 (2016).

28. Crump, M. P. *et al.* Solution structure and basis for functional activity of stromal cell-derived factor-1; dissociation of CXCR4 activation from binding and inhibition of HIV-1. *EMBO J.* **16**, 6996–7007 (1997).

29. Groeneveldt, C., van Hall, T., van der Burg, S. H., ten Dijke, P. & van Montfoort, N. Immunotherapeutic Potential of TGF-β Inhibition and Oncolytic Viruses. *Trends Immunol.* **41**, 406–420 (2020).

30. Connolly, S. A., Jardetzky, T. S. & Longnecker, R. The structural basis of herpesvirus entry. *Nat. Rev. Microbiol.* **19**, 110–121 (2021).

31. MI, K., MH, S., J, H., WT, R. & AM, A. Varicella-zoster virus (VZV) origin of DNA replication oriS influences origin-dependent DNA replication and flanking gene transcription. *Virology* **481**, 179–186 (2015).

32. Simplexvirus ~ ViralZone. https://viralzone.expasy.org/178.

33. Heldwein, E. E. & Krummenacher, C. Entry of herpesviruses into mammalian cells. *Cellular and Molecular Life Sciences* vol. 65 1653–1668 (2008).

34. Herpesvirus replication cycle ~ ViralZone. https://viralzone.expasy.org/5836.

35. Aranda, A. M. & Epstein, A. L. Latence et réactivation du virus de l'herpès simplex de type 1 (HSV-1) - Une mise à jour. *médecine/sciences* **31**, 506–514 (2015).

36. Orvedahl, A. *et al.* HSV-1 ICP34.5 Confers Neurovirulence by Targeting the Beclin 1 Autophagy Protein. *Cell Host Microbe* **1**, 23–35 (2007).

37. Li, M. & Ransohoff, R. M. Multiple roles of chemokine CXCL12 in the central nervous system: A migration from immunology to neurobiology. *Progress in Neurobiology* vol. 84 116–131 (2008).

38. Hattermann, K. *et al.* Effects of the chemokine CXCL12 and combined internalization of its receptors CXCR4 and CXCR7 in human MCF-7 breast cancer cells. *Cell Tissue Res.* **357**, 253–266 (2014).

39. CXCR4 protein expression summary - The Human Protein Atlas. https://www.proteinatlas.org/ENSG00000121966-CXCR4.

40. CXCL12 protein expression summary - The Human Protein Atlas. https://www.proteinatlas.org/ENSG00000107562-CXCL12.

41. Rempel, S. A., Dudas, S., Ge, S. & Gutiérrez, J. A. *Identification and Localization of the Cytokine SDF1 and Its Receptor, CXC Chemokine Receptor 4, to Regions of Necrosis and Angiogenesis in Human Glioblastoma*. (2000).

42. Rempel, S. A., Dudas, S., Ge, S. & Gutiérrez, J. A. Identification and localization of the cytokine SDF1 and its receptor, CXC chemokine receptor 4, to regions of necrosis and angiogenesis in human glioblastoma. *Clin. Cancer Res.* **6**, 102–111 (2000).

43. Würth, R., Bajetto, A., Harrison, J. K., Barbieri, F. & Florio, T. CXCL12 modulation of CXCR4 and CXCR7 activity in human glioblastoma stem-like cells and regulation of the tumor microenvironment. *Frontiers in Cellular Neuroscience* vol. 8 144 (2014).

44. Goffart, N., Kroonen, J. & Rogister, B. Glioblastoma-initiating cells: Relationship with neural stem cells and the micro-environment. *Cancers* vol. 5 1049–1071 (2013).

45. Signoret, N. *et al.* Phorbol esters and SDF-1 induce rapid endocytosis and down modulation of the chemokine receptor CXCR4. *J. Cell Biol.* **139**, 651–664 (1997).

46. Gatti, M. *et al.* Inhibition of CXCL12/CXCR4 autocrine/paracrine loop reduces viability of human glioblastoma stem-like cells affecting self-renewal activity. *Toxicology* **314**, 209–220 (2013).

47. Lombard, A. *et al.* The Subventricular Zone, a Hideout for Adult and Pediatric High-Grade Glioma Stem Cells. *Front. Oncol.* **10**, 3197 (2021).

48. Kaneko, N., Sawada, M. & Sawamoto, K. Mechanisms of neuronal migration in the adult brain. *Journal of Neurochemistry* vol. 141 835–847 (2017).

49. Lee, P. *et al.* Evaluation of high ipsilateral subventricular zone radiation therapy dose in glioblastoma: A pooled analysis. in *International Journal of Radiation Oncology Biology Physics* vol. 86 609–615 (2013).

50. Hallaert, G. *et al.* Survival impact of incidental subventricular zone irradiation in IDH-wildtype glioblastoma. (2021) doi:10.1080/0284186X.2021.1893899.

51. Nieszporek, A., Skrzypek, K., Adamek, G. & Majka, M. Molecular mechanisms of epithelial to mesenchymal transition in tumor metastasis. *Acta Biochimica Polonica* vol. 66 509–520 (2019).

52. Gheldof, A. & Berx, G. Cadherins and epithelial-to-mesenchymal transition. in *Progress in Molecular Biology and Translational Science* vol. 116 317–336 (Elsevier B.V., 2013).

53. Nakajima, Y. & Imanaka-Yoshida, K. New insights into the developmental mechanisms of coronary vessels and epicardium. in *International Review of Cell and Molecular Biology* vol. 303 263–317 (Elsevier Inc., 2013).

54. Atlasi, Y., Looijenga, L. & Fodde, R. Cancer Stem Cells, Pluripotency, and Cellular Heterogeneity. A WNTer Perspective. in *Current Topics in Developmental Biology* vol. 107 373–404 (Academic Press Inc., 2014).

55. Gravdal, K., Halvorsen, O. J., Haukaas, S. A. & Akslen, L. A. A switch from E-cadherin to N-cadherin expression indicates epithelial to mesenchymal transition and is of strong and independent importance for the progress of prostate cancer. *Clin. Cancer Res.* **13**, 7003–7011 (2007).

56. Loh, C. Y. *et al.* The E-Cadherin and N-Cadherin Switch in Epithelial-to-Mesenchymal Transition: Signaling, Therapeutic Implications, and Challenges. *Cells* vol. 8 (2019).

57. Musumeci, G. *et al.* Characterization of matrix metalloproteinase-2 and -9, ADAM-10 and N-cadherin expression in human glioblastoma multiforme. *Cell Tissue Res.* **362**, 45–60 (2015).

58. Klingener, M. *et al.* N-Cadherin promotes recruitment and migration of neural progenitor cells from the SVZ neural stem cell niche into demyelinated lesions. *J. Neurosci.* **34**, 9590–9606 (2014).

59. Chernoivanenko, I. S., Minin, A. A. & Minin, A. A. Role of vimentin in cell migration. *Russian Journal of Developmental Biology* vol. 44 144–157 (2013).

60. Zeng, Y. *et al.* Oncogenic ZEB2/miR-637/HMGA1 signaling axis targeting vimentin promotes the malignant phenotype of glioma. *Mol. Ther. - Nucleic Acids* **23**, 769–782 (2021).

61. BK, T., J, von E., B, K. & N, O. Two-step red-mediated recombination for versatile high-efficiency markerless DNA manipulation in Escherichia coli. *Biotechniques* **40**, 191–197 (2006).

62. Marambaud, P. *et al.* A CBP Binding Transcriptional Repressor Produced by the PS1/ϵ-Cleavage of N-Cadherin Is Inhibited by PS1 FAD Mutations. *Cell* **114**, 635–645 (2003).

63. Martínez-Martín, N., Viejo-Borbolla, A. & Alcami, A. Herpes simplex virus particles interact with chemokines and enhance cell migration. *J. Gen. Virol.* **97**, 3007–3016 (2016).

64. Viejo-Borbolla, A. *et al.* Enhancement of Chemokine Function as an Immunomodulatory Strategy Employed by Human Herpesviruses. *PLoS Pathog.* **8**, e1002497 (2012).

65. Martinez-Martin, N. *et al.* Herpes simplex virus enhances chemokine function through modulation of receptor trafficking and oligomerization. *Nat. Commun.* **6**, 1–13 (2015).

Appendices

Antibodies				
Primary antibodies				
Reactivity	**Manufacturer**	**Host**	**Assay**	**Dilution**
human Vimentin	Dako	Mouse	IF	1 : 200
HSV-1 gD	Santa Cruz	Mouse	WB	1 : 1000
HA-tag	Covance	Mouse	WB	1 : 1000
human, mouse Tubulin	DSHB	Mouse	WB	1 : 1000

Secondary antibodies					
Reactivity	**Linkage**	**Manufacturer**	**Host**	**Assay**	**Dilution**
Mouse	HRP-linked	Cell Signaling	Horse	WB	1 : 2500
Mouse	Alexa Fluor® 546	Thermo Fisher	Goat	IF	1 : 500

Table 1 : List of used antibodies.

Oligonucleotides	
By-passing cloning PCR	
Name	**Sequence 5' → 3'**
nouveau Fwd BAC-pEF1A P2G après GFP	5'-CATACACTTCATTCTCAGTATTGTTTTGCCAAGTTCTAATTCCATCAGAAGGCTCCGGTGCCCGTCAGTG -3'
inverse: Rev kanR-P2G / HA-BAC après GFP	5'-AACTTCCGGGATCAATTCATCGAAACTTAATTAACTAGAACTAGCATAACTTCGTATAATGTATGCTATACGAAGTTATTCTAGATTAAGCGTAATCTGGAACATCGTATGGGTAGTTCAGGGCCTTCTCCAGGTGCCAGTGTTACAACCAATTAACC-3'

Migration markers RT-qPCR		
Name	**Sequence 5' → 3'**	
	Hybridize to same exon	**Hybridize to different exons**
Fwd_human_vimentin	5'-CCCTCACCTGTGAAGTGGAT-3'	5'-AGCTAACCAACGACAAAGCC-3'
Rev_human_vimentin	5'-GCTTCAACGGCAAAGTTCTC-3'	5'-AGGGTGTTTTCGGCTTCCTC-3'
Fwd_human_ n-cadherin	5'-AGGATCAACCCCATACACCA-3'	5'-CAGTGCAGTCTTATCGAAGG-3'
Rev _human_ n-cadherin	5'-TGGTTTGACCACGGTGACTA-3'	5'-CCATGCCATCTTCAT CCACC-3'
Fwd_human_ e-cadherin	5'-TGCCCAGAAAATGAAAAAGG-3'	5'-CTTTGACGCCGAGAGCTACA-3'
Rev _human_e-cadherin	5'-GTGTATGTGGCAATGCGTTC-3'	5'-CCACTTTGAATCGGGTGTCG-3'

Sequencing		
Name	**Sequence 5' → 3'**	
	Forward	**Reverse**
Screening 1	5'-TGAAGTTCGAGGGCGACACCCT-3'	5'-CTCTCCCACCCACTTCCAAC-3'
Screening 2	5'-GTTGGAAGTGGGTGGGAGAG-3'	5'-ATCGCATAAAACCCCTCCCC-3'
Screening 3	5'-GGGGAGGGGTTTTATGCGAT-3'	5'-CGGTTGTTGTTCTTCAGGCG-3'
Screening 4	5'-CGCCTGAAGAACAACAACCG-3'	5'-GAGTGGGAGGAATGAGCTGG-3'

Table 2 : List of used oligonucleotides.

Polyacrylamide Gel		
Name	**Concentration (4%)**	**Separation (13%)**
Tris-HCl 1.5 M pH 8.8	-	2 mL
Tris-HCl 0.5 M pH 6.8	1 mL	-
Acrylamide 37.5/1 40% (Fisher Scientific)	400 µL	2.6 mL
H_2O	2.6 mL	3.4 mL
SDS 10%	40 µL	80 µL
APS 10%	40 µL	60 µL
TEMED (sigma)	4 µL	3 µL
Total volume	4.084 mL	8.143 mL

Table 3 : Polyacrylamide Gel composition.

Viruses				
Name	**Acronym**	**Attenuations**	**Arming**	**GFP**
fQuik1 oHSV WT-gD delta47/IE_US11 cl 2.1	oHSV	ΔICP34.5, ΔICP6, ΔICP47	Ø	✓
fQuik1 oHSV WT-gD P2G after GFP delta47/ IE_US11 cl4.3	oHSV-P2G	ΔICP34.5, ΔICP6, ΔICP47	pEF1a-P2G	✓

Table 4 : List of used viruses.

Engineering and characterization of an Oncolytic Herpes Simplex Virus type 1 armed with P2G to disrupt CXCR4 pathway in Glioblastoma Multiforme

Glioblastoma multiforme is an aggressive high-grade astrocytoma (WHO, grade IV). Current standard treatments consist in maximal surgical resection followed by chemo-/radio- therapy. Unfortunately, this treatment protocol is impaired by systematic tumour reformation. These relapses were found to be related to GSCs/GICs able to migrate from the tumour mass to the SVZ, following a CXCL12 gradient. Besides, $CXCR4^+$ GSCs are responsible, with M2-like macrophages and CAFs, for creating a particular pro-tumoral microenvironment at the tumour site driven by CXCL12/CXCR4 pathway-related autocrine and paracrine stimulation. This CXCR4/CXCL12-driven microenvironment promotes tumour cells self-renewal, proliferation, and migration, as well as tumour angiogenesis, and pro-tumoral immune modulation. Thus, GSCs and CXCL12/CXCR4 pathway became targets for new therapies against GBM recurrence and pro-tumoral microenvironment development. In this context, the injection at the tumour site of oHSV-1 expressing specific CXCL12/CXCR4 pathway inhibitors (oHSV-P2G) seems to be a potent therapeutic strategy. Through infection and continuous production of inhibitors at the tumour site, such a virus would have the potential to cause GSCs lysis, trigger inflammation against virus and tumour antigens, and disrupt the pro-tumoral microenvironment. Specifically, the aim of this master thesis is the engineering of oHSV-P2G derived from oHSV ΔICP34.5, ΔICP6, ΔICP47 and the characterisation of its effects on GSCs migration. This focus on migration follow preliminary results showing a decrease in GSCs presence, and inhibition of GBM cells stem-like features, upon inhibition of CXCL12/CXCR4 pathway using oHSV-P2G.

During this master thesis, oHSV-P2G was constructed by by-passing cloning from a BAC containing the oHSV genome and a plasmid with pEF1a-P2G sequence. Subsequently, the production of P2G and GFP by the virus were confirmed. Conditioned media containing P2G was produced and filtered. This conditioned media was used to demonstrate the effect of P2G, dissociated from potential direct effect of infection, on GSCs migration. This CXCL12/CXCR4 pathway inhibitor significatively inhibited invasion abilities of 2D human (GB138) primary GBM cells and 2D murine (GL261 N^+) GBM cells, as well as migration abilities of 3D human GBM primary cells (T013). 3D human GBM primary cells which exhibit low proportion of $CXCR4^+$ cells (T08) were used as negative control showing the specificity of the treatment towards the CXCL12/CXCR4 pathway. Nevertheless, the effect of P2G on migration could not be confirmed at the molecular level by the observation of migration markers (vimentin, cadherins).

Although these experiments have to be repeated with different cell lines, the results obtained so far are encouraging and indicate that P2G can impair GBM cells migration. The effect of oHSV-P2G on migration (as well as other features, such as stemness, angiogenesis, etc) will then be further investigated *in vivo*.

This master thesis was conducted by Maxime Dubois in the academic year 2020-2021 at the virology and immunology lab (GIGA institute) under supervision of Catherine Sadzot and Paolo D'Arrigo.